

<https://helda.helsinki.fi>

HelsinkiNet - a collaborative seismological research network of the Institute of Seismology, and the City of Helsinki

Veikkolainen, Toni

Geofysiikan seura
2022

Veikkolainen , T , Oinonen , K , Vuorinen , T , Kortström , J , Mäntyniemi , P , Lindblom , P ,
Luhta , T , Hällsten , J M A , Seipäjärvi , P J & Tiira , T 2022 , HelsinkiNet - a collaborative
seismological research network of the Institute of Seismology, and the City of Helsinki . in T
Veikkolainen , L Tuomi , T Saari , P Mäntyniemi , I Suomi , S Väkevä , A Laaksonen & L
Holappa (eds) , XXX GEOFYSIIKAN PÄIVÄT . Geofysiikan Päivät , Geofysiikan seura ,
Helsinki , pp. 65-68 , XXX Geofysiikan päivät , Helsinki , Finland , 18/05/2022 .

<http://hdl.handle.net/10138/344806>

cc_by
publishedVersion

Downloaded from Helda, University of Helsinki institutional repository.

This is an electronic reprint of the original article.

This reprint may differ from the original in pagination and typographic detail.

Please cite the original version.



GEOFYSIIKAN SEURA
GEOFYSISKA SÄLLSKAPET
GEOPHYSICAL SOCIETY OF FINLAND

XXX GEOFYSIIKAN PÄIVÄT

Helsingissä 18.-19.5.2022

Toimittaneet

Toni Veikkolainen, Laura Tuomi, Timo Saari, Päivi Mäntyniemi, Irene Suomi, Sakari Väkevä, Ari Laaksonen ja Lauri Holappa

HELSINKI 2022

ISSN 1798-2200

Julkaisu vapaasti saatavilla Geofysiikan seuran sivustolta <https://www.geofysiikanseura.fi>

Alkusanat

Geofysiikan Päivät järjestetään yleensä joka toinen vuosi, joko pääkaupunkiseudulla tai Pohjois-Suomessa. Tällä kertaa edellisistä, Rovaniemellä pidetyistä Geofysiikan Päivistä on kulunut jo kolme vuotta. Koronapandemian vuoksi Geofysiikan Päiviä ei ollut mahdollista järjestää keväällä 2021. Onneksi kuitenkin tänä vuonna saamme jälleen kokoontua tieteen ja verkostoitumisen merkeissä, tällä kertaa Helsingissä.

Geofysiikan Päivät järjestetään 18.-19.5.2022 Ilmatieteen laitoksella. Päivät järjestävät Geofysiikan Seuran puolesta Ilmatieteen laitos, Maanmittauslaitoksen Paikkatietokeskus, Helsingin yliopiston Geotieteiden ja maantieteen osasto, Suomen ympäristökeskus sekä Oulun yliopisto.

XXX Geofysiikan Päiville on ilmoittautunut 40 osallistujaa. Päivien aikana kuullaan 19 suullista esitystä ja niiden lisäksi esitellään 5 posteria. Esitelmien aihepiirit kattavat laajalti eri geofysiikan aloja.

Päivien yhteydessä jaetaan myös järjestykseltään 14. Palmén-mitali. Palmén-mitali on Geofysiikan Seuran myöntämä tunnustus henkilölle, joka on ansiokkaasti edistänyt suomalaista tutkimusta Geofysiikan Seuran edustamilla tieteenaloilla. Vuonna 2022 Palmén-mitalin saa Professori Hannu Koskinen. Tunnustuksen myöntämisen yhteydessä Prof. Koskinen luennoi aiheesta "Satunnaiskävelyllä revontulista Marsiin, Aurinkoon ja komeetan pinnalle".

Geofysiikan Seuran puolesta kiitän kaikkia, jotka ovat omalla työpanoksellaan varmistaneet XXX Geofysiikan Päivien toteutumisen.

Helsingissä 13.5.2022

Laura Tuomi

Geofysiikan seuran puheenjohtaja

Sisältö

<i>Alkusanat</i>	3
<i>XXX Geofysiikan päivien ohjelma</i>	6
<i>P. Alenius, L. Tuomi, V. González-Gambau, E. Olmedo, A. Turiel, C. González-Haro, A. García-Espriu, R. Catany ja M. Arias</i> Itämeren pintasuolaisuus satelliittihavainnoista	9
<i>M. Bilker-Koivula, T. Saari* and J. Näränen</i> Renewal of the calibration line for relative gravimeters	13
<i>F.B. Dias, P. Uotila, B. Galton-Fenzi, O. Richter, S.R. Rintoul and V. Pellichero</i> Water Mass Transformation in the Antarctic shelf	16
<i>P. Haapanala, A. Korja and FIN-EPOS, FLEX-EPOS and Nordic EPOS consortium members and working groups</i> Benefits of national and international Solid Earth Science collaboration: FIN-EPOS, FLEX-EPOS and Nordic EPOS case	17
<i>T. Hoppe, K. Kauristie, T. Laitinen and L.-P. Moisio</i> Automatic Aurora Recognition based on HSL colour ranges	21
<i>N. Junno, A. M. Rantanen, P. Bäcklund, A. Korja* and SEISMIC RISK working group</i> Geothermal energy and associated induced seismic risk management	23
<i>N. Junno, T. Luhta, K. Oinonen and T. Veikkolainen</i> Finnish National Seismic Network	27
<i>H. Kanarik, L. Tuomi, A. Westerlund ja P. Alenius</i> Saaristomeren Lövskär-Isokari väylän pohjoisosan voimakkaat virtaukset	29
<i>M. Kellinsalmi, A. Viljanen, L. Juusola and S. Käki</i> The time derivative of the geomagnetic field has a short memory	30
<i>R. Kiuru, L. Jacobsson, D. Király ja J. Suikkanen</i> Geofysiikka louhintavauriotutkimuksissa	34
<i>V. Liu, M. Nordman and N. Zubko</i> Troposphere Characterization with Space Geodetic Techniques	36
<i>T. Luhta, K. Komminaho ja P. Mäntyniemi</i> Seismisyyttä Viipurin rapakivialueella	37
<i>E. Marshalko, A. Viljanen, M. Kruglyakov and A. Kuvshinov</i> 3-D modelling of the geoelectric field in Fennoscandia with laterally nonuniform and plane wave inducing sources	41

<i>H. Pellikka, M. Johansson, M. Nordman ja K. Ruosteenoja</i>	45
Merenpinnan nousu Suomessa: historiallinen trendi ja uusimmat ennusteet	
<i>L.J. Pesonen and J. Salminen</i>	49
Ancient Supercontinents and the Paleogeography of Earth	
<i>M. Poutanen, M. Bilker-Koivula, J. Eskelinen, U. Kallio, N. Kareinen, H. Koivula, J. Näränen, J. Peltoniemi, A. Raja-Halli ja N. Zubko</i>	51
Metsähovi Geodetic Research Station	
<i>J. Salminen, S. Zhang and D.A.D. Evans</i>	55
Paleomagnetic data and the Deep-time Digital Earth program	
<i>S. Silvennoinen, J. Salminen, N. Putkinen and S. Kultti</i>	56
Ultra-high resolution sediment sequence from coastal Littorina sea spanning the Holocene thermal maximum – environmental magnetic study from Kurikka, Southern Ostrobothnia	
<i>H. Soosalu, M. Uski, K. Komminaho ja A. Veski</i>	58
Virolaisten maanjäristysten geologinen tulkinta	
<i>J. Särkkä, J. Räihä, M. Rantanen and K. Jylhä</i>	62
Simulated sea level extremes on the Finnish coast	
<i>L. Tuomi ja H. Kanarik</i>	64
Wave-induced bottom shear stress in the coastal areas of Gulf of Bothnia	
<i>T. Veikkolainen, K. Oinonen, T. Vuorinen, J. Kortström, P. Mäntyniemi, P. Lindblom, T. Luhta, J. Hällsten, P. Seipäjärvi and T. Tiira</i>	65
HelsinkiNet - a collaborative seismological research network of the Institute of Seismology, and the City of Helsinki	
<i>A. Viljanen, E. Marshalko and I. Honkonen</i>	69
Extreme geomagnetic storms in northern Europe	

* pitää esitelmän / gives the presentation

XXX Geofysiikan Päivät Helsingissä Ilmatieteen laitoksella 18.-19.5.2022

XXX Geophysics Days in Helsinki, Finnish Meteorological Institute, May 18-19, 2022

- Paikka: Dynamicum, Ilmatieteen laitos, Erik Palménin aukio 1, 00560 Helsinki
- Sivusto: <https://www.geofysiikanseura.fi>
- Osallistumismaksu: 75 € (eläkeläiset, opiskelijat ja työttömät 30 €, perustutkinto-opiskelijat ja apurahalla työskentelevät jatko-opiskelijat 10 €)
- Maksuun sisältyy: kokousohjelma, kahvitarjoilut sekä Palmén-juhlaluennon ja posterisession tarjoilu
- Esitelmät: Kokousjulkaisu on saatavissa sähköisessä muodossa päivien sivustolta kohdasta "Kokousohjelma"

Kokousohjelma keskiviikkona 18.5.2022 / Conference programme on Wednesday, May 18, 2022

9.00-9.40	Ilmoittautuminen, postereiden kiinnitys Registration, setup of posters
9.40-10.10	Kahvitauko / Coffee break
10.10-10.30	Geofysiikan päivien avaus Geofysiikan seuran puheenjohtaja
Istunto / Session 1	Puheenjohtaja / Chair: <i>Laura Tuomi</i>
10.30-10.50	<i>Mirjam Bilker-Koivula (Timo Saari*)</i> Renewal of the calibration line for relative gravimeters
	<i>Elena Marshalko</i>
10.50-11.10	3-D modelling of the geoelectric field in Fennoscandia with laterally nonuniform and plane wave inducing sources
11.10-11.30	<i>Lauri Pesonen</i> Ancient Supercontinents and the Paleogeography of Earth
11.30-11.50	<i>Heidi Soosalu</i> Virolaisten maanjäristysten geologinen tulkinta
11.50-13.00	Lounastauko / Lunch break
Istunto / Session 2	Puheenjohtaja / Chair: <i>Toni Veikkolainen</i>
13.00-13.20	<i>Havu Pellikka</i>

	Merenpinnan nousu Suomessa: historiallinen trendi ja uusimmat ennusteet
13.20-13.40	<i>Ari Viljanen</i> Extreme geomagnetic storms in Northern Europe
13.40-14.00	<i>Risto Kiuru</i> Geofysiikka louhintavauriotutkimuksissa
14.00-14.20	<i>Niina Junno (Annakaisa Korja*)</i> Geothermal energy and associated induced seismic risk management
14.20-14.50	Kahvitauko / Coffee break
Istunto / Session 3	Puheenjohtaja / Chair: <i>Johanna Salminen</i>
14.50-15.10	<i>Hedi Kanarik</i> Saaristomeren Lövskär-Isokari väylän pohjoisosan voimakkaat virtaukset
15.10-15.30	<i>Mirjam Kellinsalmi</i> The time derivative of the geomagnetic field has a short memory
15.30-15.40	<i>Johdatukset postereihin (luettelo postereista päiväohjelman lopussa)</i> <i>Introduction to posters (list of posters in the end of the daily programme)</i>
15.40-16.00	Tauko
16.00-17.00	<i>14. hopeisen Palmén-mitalin myöntäminen ja mitalistin Palmén-luento</i> <i>Awarding the 14th Palmén medal and Palmén lecture of the medalist</i>
17.00-19.00	<i>Posterit ja posteribuffet</i> <i>Posters and poster buffet</i>

* pitää esitelmän / gives the presentation

Posteresitykset / Poster presentations

P01. Päivi Haapanala
Benefits of national and international Solid Earth Science collaboration: FIN-EPOS, FLEX-EPOS and Nordic EPOS case

P02. Niina Junno
Geothermal energy and associated induced seismic risk management

P03. Niina Junno
Finnish National Seismic Network

P04. Tuija Luhta
Seismisyyttä Viipurin rapakivialueella

P05. Toni Veikkolainen
HelsinkiNet – a collaborative seismological research network of the Institute of Seismology, and the City of Helsinki

Kokousohjelma torstaina 19.5.2022 / Conference programme on Thursday, May 19, 2022

**Istunto /
Session 4** Puheenjohtaja / Chair: *Markku Poutanen*

- 10.00-10.20 *Fabio Boeira Dias*
Water Mass Transformation in the Antarctic Shelf
- 10.20-10.40 *Sonja Silvennoinen*
Ultra-high resolution sediment sequence from coastal Littorina sea spanning the Holocene thermal maximum – environmental magnetic study from Kurikka, Southern Ostrobothnia
- 10.40-11.00 *Vicky Liu*
Troposphere Characterization with Space Geodetic Techniques

11.00-11.30 Kahvitauko / Coffee break

**Istunto /
Session 5** Puheenjohtaja / Chair: *Jarkko Jokinen*

- 11.30-11.50 *Jani Särkkä*
Simulated sea level extremes on the Finnish coast
- 11.50-12.10 *Laura Tuomi*
Wave-induced bottom shear stress in the coastal areas of Gulf of Bothnia
- 12.10-12.30 *Johanna Salminen*
Paleomagnetic data and the Deep-time Digital Earth program

12.30-13.40 Lounas / Lunch

**Istunto /
Session 6** Puheenjohtaja / Chair: *Maaria Nordman*

- 13.40-14.00 *Theresa Hoppe*
Automatic Aurora Recognition based on HSL colour ranges
- 14.00-14.20 *Pekka Alenius*
Itämeren pintasuolaisuus satelliittihavainnoista
- 14.20-14.40 *Markku Poutanen*
Metsähovi Geodetic Research Station
- Nuoren tutkijan palkinnon jakaminen (palkintotoimikunnan puheenjohtaja)
Kokouksen päätäminen (Geofysiikan seuran puheenjohtaja)*
- 14.40-15.00**
- Awarding the Young Scientist's Award (chair of the award committee)
Closure of the meeting (chair of the Geophysical Society of Finland)*

Itämeren pintasuolaisuus satelliittihavainnoista

P. Alenius¹, L. Tuomi¹, V. González-Gambau², E. Olmedo², A. Turiel¹, C. González-Haro², A. García-Espriu², R. Catany³ ja M. Arias³

¹ Ilmatieteen laitos, pekka.alenius@fmi.fi

² Barcelona Expert Center ja Institute of Marine Sciences

³ ARGANS Ltd

Abstract

Remote sensing has been a standard method for observing many oceanographic parameters for decades. For the cold brackish water Baltic Sea, salinity has been the missing piece of the remote sensing routines. European Space Agency funded in 2019 – 2021 a project Baltic+ Salinity among several other projects to enhance oceanographic remote sensing. In Baltic+ Salinity under coordination of ARGANS, Barcelona Excellence Center developed proper algorithms and Finnish Meteorological Institute served expertise of in-situ conditions in the Baltic Sea. The project managed to develop two new satellite-based products that offer users gridded daily surface salinity data for years 2011 – 2019. The products have been validated by in-situ data and numerical model data and they show the general features of the salinity fields in a way that we believe to be useful for monitoring and in development of numerical models for the Baltic Sea.

1. JOHDANTO

Ensimmäinen koko Itämeren kattava suolaisuuden ja lämpötilan havainnointihanke toteutettiin 1875 ja sen tulokset julkaistiin 1893 (Ekman ja Pettersson 1893). Vuodesta 1898 Itämerta on havainnoitu systemaattisesti tutkimuslaivoilla tehdyillä havainnolla. Itämeren suolaisuuden yleispiirteet on siten tunnettu jo yli 125 vuoden ajan. Meren vesirungon tapahtumia ja ominaisuuksia on edelleen havainnoitava paikan päällä laivoilta tai automaattisilla mereen ankkuroiduilla tai meressä liikkuvilla mittalaitteilla.

Meren pinnan ominaisuuksia ja ilmiöitä on havainnoitu satelliiteista vuosikymmeniä. Merijään, pintalämpötilan ja planktonkukintojen kaukokartoitusella on pitkät perinteet. Meren pinnan suolaisuuden havainnointi satelliiteilla on ollut paljon haastavampaa. Suolaisuus on kuitenkin keskeinen suure meren dynamiikan ja eliöstön kannalta, joten se on ollut puutuva pala merten kaukokartoitusta.

Valtamereltä on jo jonkin aikaa ollut saatavissa kaukokartoituslaitteita suolaisuudesta, mutta pienet reunameret ovat olleet ongelmallisia. Meren läheisyydessä olevat maa-alueet ja talvella myös jäätä hankaloittavat signaalien tulkitsemista. Lisäksi vilkas radioliikenne saattaa

aiheuttaa häiriötä signaaliin. Itämeren ollessa kyseessä myös alhainen suolaisuus sekä lämpötila talviaikaan vaikeuttavat signaalit tulkintaa verrattuna valtameriin. Siksi satelliittihavaintoihin pohjautuvien pintasuolaisuusaineistojen käytökelpoisuus Itämereltä on ollut huono.

Euroopan Avaruusjärjestön (ESA) useiden hankkeiden kokonaisuudessa kehitettiin aikaisempaa käytökelpoisempia satelliitti havaintoihin perustuvia tuotteita Itämeren alueelle. Baltic+ Salinity Dynamics hankkeessa Barcelonan Huippututkimusyksikkö kehitti uusia algoritmeja nimenomaan Itämeren suolaisuuden määrittämiseen.

Baltic+ Salinity hankkeen ensivaiheessa tutkittiin olemassa olevien algoritmien toimintaa vuosina 2011–2013 tehtyjen satelliittihavaintojen tulkinnassa. Todettiin, että algoritmeja oli kehitettävä merkittävästi. Hankkeen aikana käytettävä satelliittiaineisto laajennettiin kattamaan vuodet 2011–2019. Vertailuhavaintoina käytettiin julkisesti saatavissa olevia Itämeren havaintoaineistoja HELCOM:n ja Kansainvälisen merentutkimusneuvoston (ICES) tietokannoista, SeaDataNet:n aineistoista ja kauppalaivoilla tehdyistä ns. Ferry Box havainnoista.

Satelliitin mittalaitteet mittaaavat hyvin ohutta meren pintafilmiä. Laivoilta tehtävät ja automaattisten mittalaitteiden havainnot ovat puolestaan pinnan alta, ylimmät havainnot 0.5–4 m syvyydeltä hieman havaintotavasta ja -instrumentista riippuen. Meren pintafilmin suolaisuudesta on saatavilla hyvin vähän suoria mittauksia ja useimmilta merialueilta niitä ei löydy lainkaan, joten ero pintafilmin ja pinnan alaisen kerroksen suolaisuudesta on tuntematon. Verratessa satelliitin tuottamaa arvoa havaintoihin joudutaan olettamaan, että pinnan suolaisuus on jokseenkin sama kuin metrin tai muutaman metrin syvyydessä olevan veden suolaisuus. Tämä on usein hyvä oletus, sillä meren pintakerros on yleensä sekoittunut useiden metrien tai kymmenten metrien syvyyteen. Itämeri on murtovesiallas, jossa suolaisuus vähenee valtamereen yhteydessä olevan eteläisen Itämeren alueen noin 12 g/kg:sta Itämeren lahtien päiden lähes makeaan veteen. Eri altaiden suolaisuus poikkeaa toisistaan ja erot ovat suurempia kuin valtameren ulapoilla alueelliset erot, jotka havainnoille asetettava tarkkuusvaatimus ei ole aivan yhtä suuri kuin valtamerien havainnoinnissa.

2. PINTASUOLAIKUUDEN MITTAUS SATELLIITISTA

Tässä esiteltävät uudet satelliittituotteet perustuvat SMOS (Soil Moisture and Ocean Salinity) satelliitin L-kaistan kirkkauslämpötilan (TB) mittauksiin. Havaintojen tulkinnan tekee haasteelliseksi monet tekniset vaikeudet, jotka liittyvät maa - meri ja jäät - meri häiriöihin, radiotaajuuskien interferenssilähteisiin ja L-kaistan kirkkauslämpötilan alhaiseen herkkyyteen pintasuolaisuuden muutoksille kylmässä vedessä sekä huonoihin dielektrisyysvakion malleihin matalan suolaisuuden ja lämpötilan oloissa. Näiden ongelmien ratkaisemiseen tehtiin projektissa paljon töitä.

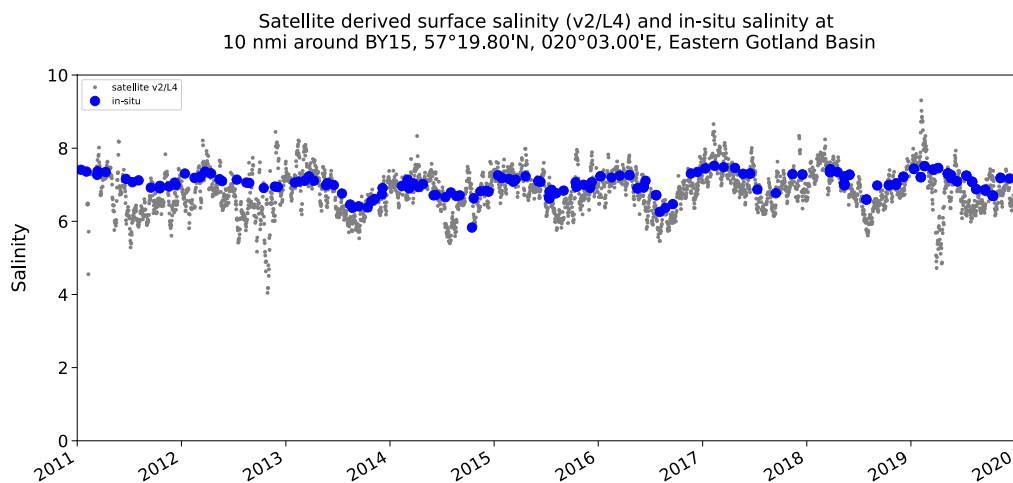
Hankkeen tuloksena kehitettiin kaksi vapaasti saatavilla olevaa satelliittituotetta. Tason 3 (L3) tuote sisältää päivittäiset 9-päivän kartat 0.25° hilassa, se löytyy Internetin osoitteesta <https://doi.org/10.20350/digitalCSIC/13859> (González-Gambau et al., 2021a). Tämän tuotteen tarkkuus suolaisuudessa on tyypillisesti noin 0.7–0.8 g/kg.

Tason 4 (L4) tuote sisältää päivittäiset kartat 0.05° hilassa ja se on saatavissa Internetin osoitteessa <https://doi.org/10.20350/digitalCSIC/13860>) (González-Gambau et al., 2021b). Tason 4 tuote on tehty yhdistämällä L3 tuotteen tiedot ja meren pintalämpötila kartat. Tämän tuotteen tarkkuus suolaisuudessa on tyypillisesti noin 0.4 g/kg.

Molempien tuotteiden tarkkuus vaihtelee merialueesta ja rannikon läheisyydestä riippuen ja suolaisuuden vaihtelu aikasarjassa on paljon suurempaa kuin suorien havaintojen aikasarjoissa. Pienet osa-altaat, kuten Arkonan ja Bornholmin altaat ja Riianlahti sekä Suomenlahti ovat edelleen haasteellisia ja niissä tarkkuus on pienempi.

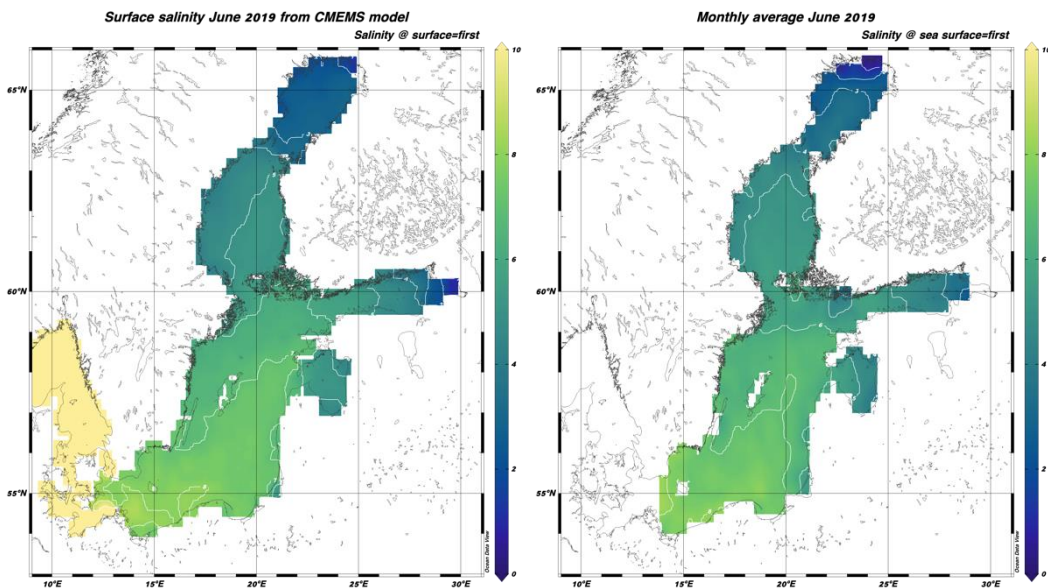
3. TUOKSET

Tässä näytämme esimerkin satelliitista mitatusta pintasuolaisuuden aikasarjasta keskeltä Itämerta Gotlannin syvanteelta (Kuva 1). Kuvaan on piirretty päivittäiset satelliittihavainnoista tulkitut pintasuolaisuudet harmaina pisteinä ja saman alueen havaintopisteeltä BY15 laivalta ns. CTD-luotaimella mitatut suolaisuudet. Havaintopiste BY15 on sellainen avomeren piste, jossa tehdään paljon havaintoja. Vertailusta havaitaan, että satelliittihavaintojen hajonta on huomattavasti suurempi kuin laivahavaintojen. Satelliittihavaintojen yleispiirteet, kuten vuosien välinen ja vuodenaikaisvaihtelut, ovat kuitenkin samankaltaisia laivahavaintojen kanssa.



Kuva 1: Satelliitti havainnoista johdettu pintasuolaisuus (harmaa pisteet) ja laivalta mitattu suolaisuus (siniset pisteet) Itämeren keskiosasta Gotlannin itäpuolen havaintopisteeltä BY15).

Satelliittihavaintojen karttamuotoista esitystä on verrattu numeeristen mallien tuottamiin pintasuolaisuuden karttoihin. Suuria havaintoja on yleensä niin vähän, että niiden tuottamat karttaesitykset ovat epätarkkoja, mutta niin ovat sekä numeeristen mallien tuottamat, että satelliittihavaintojen tuottamat kartatkin. Vertailu osoittaa, että pintasuolaisuuden yleispiirteet näyttävät samankaltaisilta.



Kuva 2: Yleisen Eurooppalaisen CMEMS palvelu numeerisen mallin tuottama pintasuolaisuuskartta (vasemmalla) ja satelliittihavaintojen tuottama pintasuolaisuuskartta (oikealla). Molemmat edustavat kesäkuun 2019 keskiarvoa.

KIITOKSET

Työ on tehty Euroopan avaruusjärjestön ESAn rahoittamassa hankkeessa Baltic+ Salinity Dynamics (4000126102/18/I-BG).

LÄHTEET

González-Gambau, V., E. Olmedo, C. González-Haro, A. García-Espriu, and A. Turiel, 2021a. Baltic Sea Surface Salinity L3 maps, <https://doi.org/10.20350/digitalCSIC/13859>.

González-Gambau, V., E. Olmedo, C. González-Haro, A. García-Espriu, and A. Turiel, 2021b. Baltic Sea Surface Salinity L4 maps, <https://doi.org/10.20350/digitalCSIC/13860>.

González-Gambau, V., E. Olmedo, A. Turiel, C. González-Haro, A. García-Espriu, J. Martínez, P. Alenius, L. Tuomi, R. Catany, M. Arias, C. Gabarró, N. Hoareau, M. Umbert, R. Sabia, and D. Fernández, 2022. First SMOS Sea Surface Salinity dedicated products over the Baltic Sea, *Earth System Science Data*, accepted in press, <https://doi.org/10.5194/essd-2021-461>.

Renewal of the calibration line for relative gravimeters

M. Bilker-Koivula¹, T. Saari¹ and J. Näränen¹

Maanmittauslaitos, Paikatietokeskus FGI, mirjam.bilker-koivula@maanmittauslaitos.fi

Abstract

In this article, we describe the renewal of the calibration line for relative gravimeters that is maintained by the National Standard Laboratory for free-fall acceleration of the Finnish Geospatial Research Institute (FGI), National Land Survey of Finland. From 1997 onwards the line has been situated between the Masala end station and the Vihti end station. In May 2022, with the move of the FGI to its new office on the Otaniemi campus in Espoo, came the need to renew the calibration line and move the southern end station from the Masala office to the new Otaniemi office. We describe the absolute and relative gravity measurements done for the renewal. New gravity values for the end stations of the calibration line will be made public in June 2022 and for the relative stations in between in the autumn of 2022.

1. INTRODUCTION

Since 1959 the Finnish Geodetic Institute has maintained a calibration line for gravimeters (Kiviniemi, 1963; 1964). From 1997 onwards the Masala-Vihti calibration line has been in use (Ruotsalainen et al. 1998). One end station of this line is situated in Olkkala, in the municipality of Vihti, and the other end station in the office of the Geospatial Research Institute of the National Land Survey, FGI (former Finnish Geodetic Institute) in Masala, in the municipality of Kirkkonummi. On May 1st, 2022, the office of FGI moved to a new location on the Otaniemi Campus in Espoo. This created a need for a reformation of the line. Here we will introduce the current calibration line, its renewal, and the schedule of the renewal.

2. THE MASALA-VIHTI CALIBRATION LINE

The Masala-Vihti calibration line for relative gravimeters was established in 1997 by the FGI, after the FGI had moved to the Masala office in Kirkkonummi. Nowadays the line is maintained by the National Standards Laboratory for free-fall acceleration, which belongs to the Department of Geodesy and Geodynamics of the FGI.

Originally the southern end point of the line was situated inside in the gravity laboratory that contained four pillars that were based on bedrock, with the main station being Masala AA (961002). The construction of these pillars was not satisfactory and in 2006 the gravity laboratory was moved to a new location within the building and two new pillars, Masala AB

and Masala AC, were established on bedrock. For practical use point 971007 was established already from the start outside the building. Point 971007 can easily be accessed without making arrangements with the gravity laboratory. Also, possible temperature gradient effects on the gravimeters, caused by indoor and outdoor temperature differences, can be avoided when starting the relative gravity measurements on the calibration line from the point outside.

The northern end point of the line is situated in Olkkala, Vihti. This station Vihti AA (971012) is on a low concrete base, which was established on a small bedrock exposure. A roof was built over the pillar for protection from the weather. For absolute gravity measurements temporary walls of plywood board are put up to be able to create the necessary stable temperature.

Both end points have been measured several times with an absolute gravimeter: In 1997 with the JILAg-5 of the FGI, in 2008 with the FG5-221 and in 2014 and 2019 with the FG5X-221. The FG5(X)-221 is the national standard for the acceleration of free-fall and measurements by this instrument can be directly traced to the SI standards for length and time.

In between the end stations four easily accessible points (971008, 971009, 971010, 971011), with gravity differences of about 10 mGal between them, were established using relative gravimeters.

Ruotsalainen et al. (1998) gives an extensive overview of the Masala-Vihti calibration line including the results of the 1997 measurements with gravity values for all points of the line.

2. RENEWAL OF THE CALIBRATION LINE

In spring 2022 the southern end station of the calibration line is moved from the old FGI building in Masala to the new building in Otaniemi: Vuorimiehetie 5, Espoo. The new end station Otaniemi AA (2022001) will be established on a specially constructed pillar in the new extension on the back side of the office building. The pillar is situated in a maintenance pit below the floor in the garage of the building. Also here, a point (2022002) will be established outside of the building for easy access.

The northern end station of the line will continue to be the station Vihti AA (971012). The relative points in between, 971008, 971009, 971010 and 971011, will be checked and if needed a new point will be established between point 2022002 and 971008.

In May 2022 absolute gravity measurements are performed with the FG5X-221 at the old and new end stations, Masala AB and AC, Vihti AA and Otaniemi AA, and relative gravity measurements will take place in Otaniemi between the station AA (2022001) inside and the point outside (2022002). Also, the gradient at Otaniemi AA will be determined. In June 2022 relative gravity measurements will take place between the end points 2022002 and Vihti AA (971012), also visiting the relative points in between.

3. OUTLOOK

In June 2022 we will issue measurement certificates for the absolute gravity measurements at the stations Otaniemi AA (2022001) and Vihti AA (971012) and publish the gravity values of

these stations as well as the gravity value of the outdoor point 2022002 together with a site description. Gravity values for all the points in the calibration line will be published in the autumn of 2022. It is anticipated that the gravity values of the renewed calibration line will be published on the website of the National Land Survey.

We plan to repeat the absolute gravity measurements at Otaniemi AA and Vihti AA in the first half of 2023. In the future absolute gravity measurements at these stations will take place every five years.

The old outdoor point 971007 in Masala can still be used as long as it is available until the values of the new points have been made public. With questions related to the calibration line or the national gravity standard you can contact the National Standards Laboratory for Free-fall Acceleration via email at the following address: FGI_KML_Putoamiskihtyyvys@nls.fi

REFERENCES

- Kiviniemi, A., 1963. Om kalibreringslinjer vid de finska tyngkraftmätningarna. Protokoll, Nordiska Kommissionen för Geodesi, Det Fjerde Nordiske Geodetmøte, 14-18 mai 1962, pp. 177-180. Norges Geografiske Oppmåling, Oslo
- Kiviniemi, A., 1964. The first order gravity net of Finland. *Publications of the Finnish Geodetic Institute*, **59**. Helsinki
- Ruotsalainen, R., J. Mäkinen ja J. Kääriäinen, 1998. Gravimetrien kalibrointilinja Masala-Vihti. *Suomen geodeettisen laitoksen tiedote*, **20**. Masala.

Water Mass Transformation in the Antarctic shelf

F.B. Dias¹, P. Uotila¹, B. Galton-Fenzi², O. Richter³, S.R. Rintoul⁴ and V. Pelichero⁵

¹ Institute for Atmospheric and Earth System Research (INAR), fabio.boeiradias@helsinki.fi

² Institute for Marine and Antarctica Studies, University of Tasmania, Hobart, Tasmania, Australia

³ Alfred Wegener Institute for Polar and Marine Research, Bremerhaven, Germany

⁴ CSIRO Oceans and Atmosphere, Hobart, Tasmania, Australia

⁵ Ifremer Centre de Bretagne: Plouzane, Bretagne, France

Abstract

Antarctic Bottom Water (AABW) forms around Antarctica, sinks to the ocean's abyss and fills more than 30% of the ocean's volume. The formation of AABW includes mixing of distinct water masses, such as High Salinity Shelf Water (HSSW), Ice Shelf Water (ISW) and Circumpolar Deep Water on the continental shelf. Despite its climatic importance, the mechanisms of AABW formation are poorly known due to the lack of observations and the inability of climate models to simulate those mechanisms. We applied the Water Mass Transformation (WMT) framework in density space to simulations from a circumpolar ocean-ice shelf model (WAOM/Whole Antarctic Ocean Model, with horizontal resolution ranging from 10 to 2 km) to understand the role of surface fluxes and oceanic processes to water mass formation and mixing on the Antarctic continental shelf, including the ice shelf cavities. The salt budget dominates the water mass transformation rates, with only secondary contribution from the heat budget. The buoyancy gain at light density classes ($27.2 < \sigma_0 < 27.5 \text{ kg m}^{-3}$) is dominated by basal melting. At heavier densities ($\sigma_0 > 27.5$), salt input associated with sea-ice growth in coastal polynyas drives buoyancy loss. The formation of HSSW occurs via diffusion of the surface fluxes, but it is advected towards the cavities of large ice shelves (e.g., Ross, Filchner-Ronne), where it interacts with ice shelf through melting and refreezing and forms ISW. The sensibility of those mechanisms to the model horizontal resolution was evaluated. The basal melting and associated buoyancy gain rates decrease with increased resolution, while buoyancy loss associated with coastal polynyas are less sensible to resolution as surface fluxes are estimated from sea ice concentration observations. These results highlight the importance of high resolution to accurately simulate AABW formation, where mixing processes occurring below ice shelf cavities play a key role in WMT.

Benefits of national and international Solid Earth Science collaboration: FIN-EPOS, FLEX-EPOS and Nordic EPOS case

**P. Haapanala¹, A. Korja¹, and FIN-EPOS, FLEX-EPOS and Nordic EPOS consortium
members and working groups**

¹ Institute of Seismology, University of Helsinki, fin-epos@helsinki.fi

Abstract

The European Plate Observing System (EPOS) is a multidisciplinary research infrastructure that facilitates the long-term integration of data, services and facilities for solid Earth science in Europe. Finland's participation in EPOS is coordinated by FIN-EPOS consortium that is a joint community of universities and research institutes with tasks of maintaining geophysical observatories and laboratories in Finland. Finland has also active role in Nordic capacity building and knowledge exchange related to EPOS and in particular (meta)data management. International collaboration supports the availability, recognition and FAIRness of Nordic EPOS related data.

1. INTRODUCTION

What is a research infrastructure and why there is a need for several different pan-European research infrastructures? We cover shortly the general concept of a research infrastructure (RI) and concentrate on particular in the European Solid Earth Science RIs and to national and Nordic collaboration around them.

A research infrastructure can refer to instruments, equipment, information networks, databases, materials and services. RI enables the research community to use specific facilities, resources, and services in order to conduct research, foster innovations and promote sustainable research and research collaboration. European Strategy Forum on Research Infrastructures (ESFRI) supports coherent and strategy-led approach to policy-making on RIs in Europe with a mandate from the EU Council. It also facilitates multilateral initiatives leading to the better use and development of RIs, at EU and international level. ESFRI selects proposals of RIs in strategic areas of research and with an adequate level of maturity to become ESFRI Projects, and identifies successfully implemented RIs to become ESFRI Landmarks.

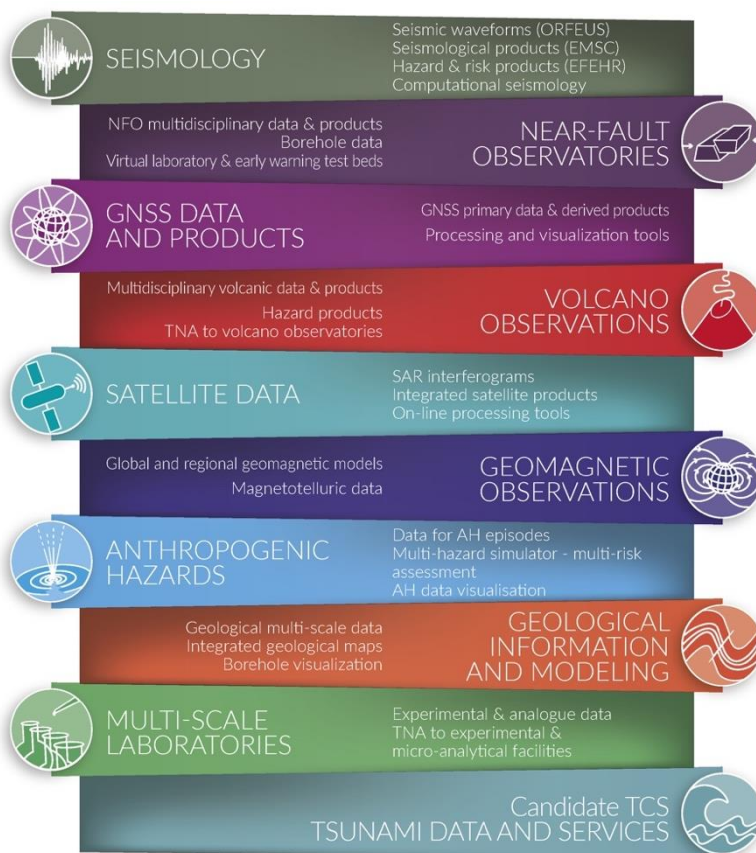
2. EUROPEAN PLATE OBSERVING SYSTEM

European Plate Observing System, EPOS (epos-eu.org), is a multidisciplinary, distributed RI in the Solid Earth Science domain and it is one of the ESFRI landmark RIs (Cocco et al., 2022; Cocco and Montone, 2022). EPOS is a long-term plan for the integration of existing national

and transnational RIs for solid Earth Science in Europe. The European Commission granted the legal status of European Research Infrastructure Consortium (ERIC) to EPOS in 2018. EPOS ERIC, based in Italy, is currently joined by fourteen countries: Belgium, Denmark, France, Greece, Iceland, Italy, the Netherlands, Norway, Poland, Portugal, Romania, Slovenia and the United Kingdom, and Switzerland participating as observer (Atakan et al., 2022). Sweden and Finland are foreseen to join EPOS ERIC during this and next year. Furthermore, many other European countries are involved in EPOS by providing data, data products, software, and/or services to be integrated by 10 thematic subdisciplines of solid Earth science. National governments, funding agencies and institutes are responsible for the funding and operation of national instrumentation and data management in each participating country.

The EPOS overarching goal is to establish a comprehensive multidisciplinary research platform and principal source of geoscientific data, metadata and tools of Solid Earth in Europe. The EPOS Framework can be defined as a truly international, federated framework encompassing the data and service provision integrated within the Thematic Cores Services (TCS) and made interoperable with the central hub of the Integrated Core Services (ICS-C), the novel e-infrastructure for promoting FAIR (Findable, Accessible, Interoperable, and Reusable) data management. The community-specific TCS are listed in Figure 1.

Figure 1: EPOS service integration plan. There are 10 subdiscipline specific Thematic Core Services (TCS) currently integrated in EPOS: Seismology, Near-Fault Observatories, GNSS Data and Products, Volcano observations, Satellite Data, Geomagnetic Observations, Anthropogenic Hazards, Geological Information and Modelling, Multi-Scale Laboratories. TCS Tsunami Data and Services is a new candidate to become EPOS TCS. (Figure ©EPOS ERIC)



3. FIN-EPOS (helsinki.fi/en/infrastructures/fin-epos)

The Finnish national node of EPOS is called FIN-EPOS (Atakan et al, 2022). FIN-EPOS is a joint community of universities and research institutions: University of Helsinki (UH),

University of Oulu (OUULU), Aalto University (Aalto), National Land Survey (NLS, FGI), Finnish Meteorological Institute (FMI), Geological Survey of Finland (GTK), VTT Technical Research Center for Finland Ltd (VTT), and CSC- IT Centre for Science Ltd (CSC). FIN-EPOS is on the national roadmap of research infrastructures in Finland 2021–2024.

FIN-EPOS partners own and operate national Earth science research infrastructures including geophysical and geodetic observatories, and laboratories. These RIs consist of physical measurement instrumentation and stations as well as associated data centers, services and personnel. The permanent seismic, geodetic and magnetic observatory networks are distributed around Finland, whereas the geophysical, geodynamic and petrophysical laboratories are located in Helsinki, Espoo, Kuopio, Rovaniemi, Kirkkonummi, Oulu and Pyhäsalmi (Calliolab). Partners own their (meta)data and deliver or are preparing for delivering it to the EPOS TCS through national nodes, international data centers or global scientific programs.

FIN-EPOS has a coordination office at the Institute of Seismology, University of Helsinki, and a council that is responsible for defining a long-term national solid Earth sciences RI plan. The council monitors and supports partners data delivery to EPOS TCSs and establishing transnational access. The council is also responsible for enhancing Finnish participation at initiatives related to EPOS, increasing the user base of EPOS data, both nationally and internationally. FIN-EPOS activities are financed by host organizations that in turn are government research organizations financed by five ministries: Ministries of Education and Culture, Agriculture and Forestry, Employment and the Economy, Transport and Communications, and Foreign Affairs. FIN-EPOS received Academy of Finland FIRI funding for 2021-2024 to support national co-ordination. National governmental process for Finland to join EPOS ERIC as a member country is ongoing.

During the past few years, FIN-EPOS has been upgrading the Finnish National Seismological Network (FNSN), and the geodetic and magnetic networks and laboratories. Currently, FIN-EPOS is enhancing measurement site collaboration. Sharing station infrastructure and deploying several independent measurement instruments on a single site enables not only new studies on the interdependencies of the seismic, geomagnetic and geodetic processes but also usage as reference stations, ground truth stations for mobile instruments and airborne measurements. These so-called **geophysical superstations with co-located instruments** will be developed around already existing geophysical observatories and station networks. FIN-EPOS is also taking part in collaboration with other national nodes of environmental ESFRI RIs in establishing joint geophysical and environmental superstations.

For more information on EPOS in general and national EPOS activities and data, can be found on the FIN-EPOS website helsinki.fi/en/infrastructures/fin-epos. Via website you find links to online databases of the Finnish geophysical and geodetic observatories and laboratories: Earthquake bulletins, FIRE data, Paleomagia, spatial data products via Hakku (GTK), Sodankylä Geophysical Observatory data (SGO/OUULU), data from magnetometer stations via IMAGE (International Monitor for Auroral Geomagnetic Effects). There are also links to EPOS related databases in Norden (helsinki.fi/en/infrastructures/nordic-epos/databases) and of course link to access the EPOS data portal (epos-eu.org/dataportal).

4. FLEX-EPOS (wiki.helsinki.fi/display/FLEX/Flex-epos+Home)

The latest Academy of Finland FIRI funded EPOS RI project is FLEX-EPOS - *Flexible instrument network for enhanced geophysical observations and multi-disciplinary research*. The FLEX-EPOS consortium includes FIN-EPOS partners UH, UOULU, GTK, FGI, Aalto, and VTT and external partner University of Turku (UTU). The objective of FLEX-EPOS is to create a national pool of mobile geophysical instruments and to build multi-disciplinary geophysical superstations. FLEX-EPOS seismic instrument pool is hosted by UH and the instruments and services of the pool are available for members of the partner organizations and collaboration partners. For more details on the project including pool instrumentation, application process, fees and liabilities, see FLEX-EPOS wiki pages (wiki.helsinki.fi/display/FLEX/Flex-epos+Home).

5. NORDIC EPOS (www2.helsinki.fi/en/infrastructures/nordic-epos)

EPOS related cooperation is especially important in bringing forward Nordic common research interests in georesources and in the Nordic natural phenomena such as postglacial uplift, geomagnetic storms, and seismic hazard in low seismicity intraplate areas. UH is leading a NordForsk funded Nordic EPOS consortium that support Nordic collaboration by organizing workshops, trainings and events on EPOS data usage, FAIR data principles, and on harmonizing data management. Nordic EPOS activities are aimed for students, researchers, and technical staff working in Nordic countries in the field of Solid Earth Sciences. More information on Nordic EPOS collaboration, activities and links to EPOS related data are available on the Nordic EPOS website www2.helsinki.fi/en/infrastructures/nordic-epos.

ACKNOWLEDGEMENTS

The national FIN-EPOS coordination and participation in EPOS ERIC and FLEX-EPOS have been granted with FIRI funding from the Academy of Finland for 2021–2024 by funding decisions 328984 and 328776, 328778-328782, 328784, 328786. Nordic EPOS – A FAIR Nordic EPOS Data Hub -project receives financial support from the NordForsk Research Infrastructure Hubs 2020–2022 call, decision number 97318.

REFERENCES

- Cocco, M., C. Freda, K. Atakan, D. Bailo, K.S. Contell, O. Lange, and J. Michalek, 2022. The EPOS Research Infrastructure: a federated approach to integrate solid Earth science data and services. *Annals of Geophysics*, **65**, 2, DM208; doi.org/10.4401/ag-8756
- Cocco, M., and P. Montone, 2022. EPOS a Research Infrastructure in solid Earth: open science and innovation. *Annals of Geophysics*, **65**, 2; doi.org/10.4401/ag-8835
- Atakan, K, M. Cocco, B. Orlecka-Sikora, R. Pijnenburg, J. Michalek, C. Rønnevik, D. Olszewska, B. Górką-Kostrubiec, and M.R. Drury, 2022. National EPOS initiatives and participation to the EPOS integration plan. *Annals of Geophysics*, **65**, 2, DM211; doi.org/10.4401/ag-8758

Automatic Aurora Recognition based on HSL colour ranges

T. Hoppe¹, K. Kauristie¹, T. Laitinen¹ and L.-P. Moisio¹

¹ Finnish Meteorological Institute, theresa.hoppe@fmi.fi

Abstract

We develop a real-time capable method for automatically recognising auroras in all-sky camera (ASC) colour images. A fast image recognition algorithm allows to build a nowcast service based on ASC data with a higher accuracy compared to nowcasts based on geomagnetic proxies. We classify all pixels in an image based on their HSL (Hue-Saturation-Lightness) values into two groups: aurora and no-aurora. Furthermore, we find a global threshold value that defines the minimum number of aurora pixels required to assign the image to the aurora category. In the presentation we describe the details of our classification method and present some preliminary results from its validation.

1. INTRODUCTION

Automated digital cameras equipped with fish-eye lenses are operated at auroral latitudes by several research institutes both for scientific purposes and to support auroral tourism. On the Northern hemisphere imaging season extends typically from September to April. During such a season a camera taking images with a 10 sec cadence produces easily more than 600 000 images. Auroras appear only in a fraction of those images and pruning them out from the massive data archive for further analysis is a challenge which requires automatic categorisation routines. Promising results have been achieved with machine vision approaches that recognize auroral structures from all-sky camera images (Syrjasuo and Partamies, 2012; Rao et al., 2014). These routines are accurate but require careful training of the routines by an experienced scientist.

We present an alternative approach for ASC data pruning, which as a simple and transparent solution is suitable for near-real-time services supporting auroral tourism. The proposed approach analyses individual pixels in colour images. Besides binning the pixels into the two main groups (aurora and no-aurora) our goal is to characterise automatically also the background conditions (clouds, clear sky, moon).

2. THE ALGORITHM

The pixel categorisation is based on HSL values. We define minimum and maximum values for H, S and L and apply those as a threshold to each pixel in an image. If the H, S and L

values of the pixel are within the HSL ranges, the pixel is classified as aurora. If one or more values are outside of the HSL ranges, the pixel is classified as no-aurora (Fig. 1).

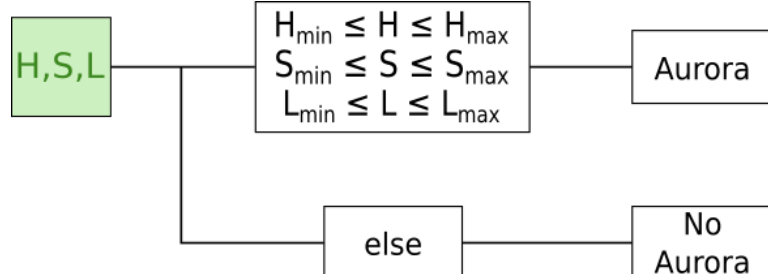


Figure 1: Schematic presentation of the pixel categorisation

ASC data is stored in AVI format. We extract individual frames from the video at a resolution of 1 frame per minute. The frame is transformed from RGB (red-green-blue) colour space to HSL colour space and a mask is applied to the image to cut away trees and other objects at the horizon. The image is cropped to the size of the mask to reduce the number of pixels that are processed. Each pixel is assigned to a category (Figure 2) and subsequently a global threshold is applied to the number of aurora pixels. If the number of aurora pixels is greater than or equal to 10% of the total number of pixels, the image is classified as aurora. Otherwise the image is categorised as no-aurora.

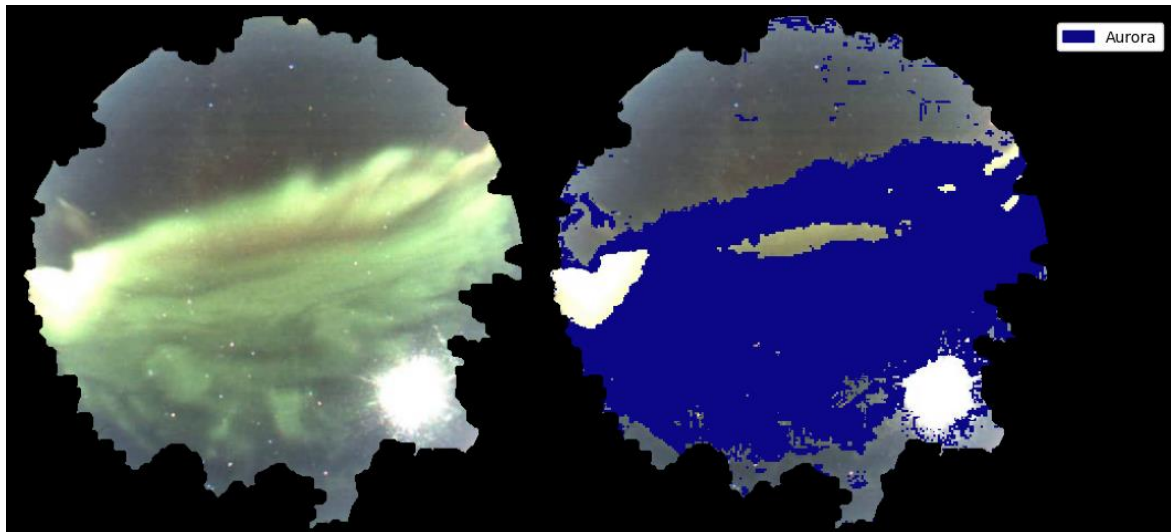


Figure 2: Masked and cropped All-sky camera image on the left. Pixel categorisation on the right. Aurora pixels are marked in blue.

REFERENCES

- Rao, J., N. Partamies, O. Amariutei, M. Syrjäsuo, and K.E.A. van de Sande, 2014. Automatic Auroral Detection in Color All-Sky Camera Images. *IEEE Journal of Selected Topics in Applied Earth Observations and Remote Sensing*, **7**, 4717-4725.
- Syrjäsuo, M., and N. Partamies, 2021. Numeric Image Features for Detection of Aurora. *IEEE Geoscience and Remote Sensing Letters*, **9**, 176-179.

Geothermal energy and associated induced seismic risk management

N. Junno¹, A. M. Rantanen¹, P. Bäcklund¹, A. Korja¹ and SEISMIC RISK working group

¹ Department of Geosciences and Geography, University of Helsinki, niina.junno@helsinki.fi

Abstract

SEISMIC RISK – mitigation of induced seismic risk in urban environment – project studies how to evaluate, mitigate, communicate, and govern induced seismic risk associated with deep geothermal energy production. The research consortium consists of the University of Helsinki, VTT Technical Research Center of Finland and Geological Survey of Finland. As part of the research objectives, the project aims to increase the awareness and understanding of induced seismic risk among different stakeholders, and to improve understanding of the complexities of decision-making process and the inclusion and roles of different actors.

1. INTRODUCTION

Deep geothermal energy has a huge potential as environmentally friendly carbon-free district heat source in urban centers in Finland. Currently, there are several geothermal projects ongoing and in planning. One of the risks associated with geothermal energy is that it may induce small-magnitude earthquakes posing a risk to critical sensitive infrastructure. As geothermal energy is a relatively new way to produce energy in Finland, the administrative norms and arrangements are being formulated as the technology is being tested. One of the goals of the SEISMIC RISK project is to facilitate the development of uniform permitting and regulation for the geothermal energy sector.

2. ONGOING GEOTHERMAL PROJECTS IN FINLAND AND ASSOCIATED INDUCED SEISMICITY

The first pilot geothermal project in Finland was the St1 Deep Heat project in Otaniemi, Espoo. The aim of the Otaniemi project was to test the applicability of Enhanced Geothermal System (EGS) in Finnish bedrock conditions. The drilling of the EGS wells started in 2016. The wells, with the depth of approximately 6400 m, were stimulated in 2018 and 2020 to enhance the water circulation within the bedrock. These stimulations induced several hundreds of small-magnitude earthquakes that were recorded by seismic stations installed for monitoring purposes around the site (Uski & Piipponen 2019, Hillers et al. 2020, Rintamäki et al. 2021, and Veikkolainen et al. 2021). The largest of the induced earthquakes were felt, heard, and reported by the citizens to the Institute of Seismology, University of Helsinki.

Based on the stimulation test results, the energy companies concluded that Otaniemi EGS would not be profitable district heat source and ST1 closed down the operations late 2021.

At Koskelo, Espoo, QHeat started drilling a medium deep (1300 m) geothermal single well in summer 2016. The operation at the geothermal plant started in 2020. The Koskelo geothermal well had been located close to a major structural zone, Porkkala-Mäntsälä fault zone. In December 2020, a M1.1 earthquake occurred at Koskelo, Espoo, at close vicinity to the geothermal well, and it was classified as a probably induced earthquake (Veikkolainen et al. 2021). In addition to these two pilot projects, several medium deep and deep geothermal projects, as well as shallow borehole heat exchanger fields, are in the planning in Finland.

3. SEISMIC HAZARD AND RISK

Seismic hazard represents the best possible estimate of the level of seismicity in a given target region in a given time period. The level of seismic hazard cannot be altered by human activities. Seismic risk (Figure 1) describes the impact of the seismic hazard on build infrastructures and human wellbeing. It consists of the seismic hazard and seismic vulnerability, exposure and costs associated with earthquake consequences. The level of seismic risk can be mitigated by, e.g., mitigating seismic vulnerability (i.e., constructing buildings that perform well during earthquake ground shaking).

$$\text{Seismic Risk} = \text{Seismic Hazard} \times \left(\begin{array}{c} \text{Exposure and Vulnerability} \\ + \\ \text{Local Soil Conditions} \\ + \\ \text{Value Concentration} \end{array} \right)$$

Figure 1: A probabilistic seismic risk analysis is a product of seismic hazard and the fragility of the environment. This fragility can include different factors such as exposure, vulnerability, soil conditions, and sometimes cost is added (adapted from Crowley et al. 2021, and Danciu et al. 2021).

4. RISK MANAGEMENT

Large-scale geothermal energy is a relatively new technology, meaning that there is little experience in regulating, building, and operating the infrastructure. There are many stakeholders at various levels, from local to national, that have diverging and perhaps conflicting interests and agendas. In 2021, as part of the SEISMIC RISK project, interviews were conducted on the current state of seismic risk management in Finland. Based on the interviews, the aspects of different stakeholders on who should be involved in risk management and what kind of information different parties feel they need for risk management were analyzed (Tuomisaari et al. in review). The key finding was that the perceptions of the nature of the risk and the hazard and the respective roles of different actors and the need for regulation vary (Tuomisaari et al. in review). There were also different interpretations concerning what kind of knowledge is needed for risk management.

Since the beginning of the SEISMIC RISK project, several advancements have been made in the geothermal energy sector related to the awareness of the induced seismic risk (Figure 2).

The Ministry of Economic Affairs and Employment launched in 2022 an investigation on the legislative needs and potential of geothermal energy in Finland. Large cities together with the Institute of Seismology, University of Helsinki have initiated a discussion forum to exchange information on the progress of geothermal projects and to facilitate information distribution in urban planning, permitting and technical expertise of geothermal projects.

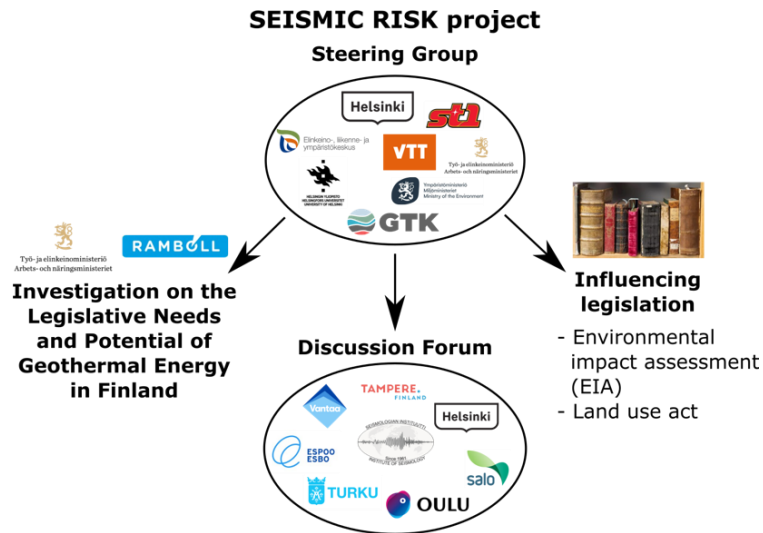


Figure 2: SEISMIC RISK project is involved in several stakeholder discussion forums to increase the awareness of increased seismic risk around deep geothermal energy sites and to facilitate the development of uniform permitting and regulation for the geothermal energy industry.

ACKNOWLEDGEMENTS

SEISMIC RISK project is funded through Academy of Finland's special funding for Crisis preparedness and security of supply (project number 337913) during 8/2020-11/2023.

REFERENCES

- Crowley, H., J. Dabbeek, V. Despotaki, D. Rodrigues, L. Martins, V. Silva, X. Romão, N. Pereira, G. Weatherill, and L. Danciu, 2021. European Seismic Risk Model (ESRM20), EFEHR Technical Report 002, V1.0.1, 84 pp, <https://doi.org/10.7414/EUC-EFEHR-TR002-ESRM20>
- Danciu L., S. Nandan, C. Reyes, R. Basili, G. Weatherill, C. Beauval, A. Rovida, S. Vilanova, K. Sesetyan, P.-Y. Bard, F. Cotton, S. Wiemer, and D. Giardini, 2021. The 2020 update of the European Seismic Hazard Model: Model Overview. EFEHR Technical Report 001, v1.0.0, <https://doi.org/10.12686/a15>
- Hillers, G., T.A.T. Vuorinen, M. Uski, J. Kortström, P. Mäntyniemi, T. Tiira, P.E. Malin, and T. Saarno, 2020. The 2018 Geothermal Reservoir Stimulation in Espoo/Helsinki, Southern Finland: Seismic Network Anatomy and Data Features. *Seismological Research Letters*, 91(2), 770–786. <https://doi.org/10.1785/0220190253>

Rintamäki, A.E., G. Hillers, T. Vuorinen, T. Luhta, J. Pownall, C. Tsarsitalidou, K. Galvin, J. Keskinen, J. Kortström, T.-C. Lin, P. Mäntyniemi, K. Oinonen, T.J. Oksanen, P.J. Seipäjärvi, G. Taylor, M. Uski, A.I. Voutilainen, and D. Whipp, 2021. A seismic network to monitor the 2020 EGS stimulation in the Espoo/Helsinki area, southern Finland. *Seismological Research Letters*, **93(2A)**, 1046–1062. <https://doi.org/10.1785/0220210195>

Tuomisaari, J., N. Junno, P. Bäcklund, and A. Korja (in review). Geotermisen energian ja poliittikkaongelmien hallitsemisen tiedollinen haaste. *Alue & Ympäristö*.

Uski, M., and K. Piipponen, (Eds.), 2020. Report on deep hole drilling in geothermal energy projects, associated environmental perspectives and risk management: Guidelines for permit authorities. *Report S-70, Institute of Seismology, University of Helsinki*, <http://hdl.handle.net/10138/313884>

Veikkolainen, T., K. Oinonen, T. Vuorinen, J. Kortström, P. Mäntyniemi, P. Lindblom, M., Uski, and T. Tiira, 2021. Helsingin seisminen asemaverkko ja seismisyys 2020. *Report T-103, Institute of Seismology, University of Helsinki*, <http://hdl.handle.net/10138/326738>

Finnish National Seismic Network

Niina Junno¹, Tuija Luhta¹, Kati Oinonen¹ and Toni Veikkolainen¹

¹ Institute of Seismology, Department of Geosciences and Geography, University of Helsinki,
niina.junno@helsinki.fi

Abstract

The role of the Finnish National Seismic Network (FNSN) is to record seismic signals from earthquakes, explosions and other seismic events in order to identify, locate and determine the magnitudes of the events. A comprehensive national seismic network is essential for seismological research, observational activities, and government regulations for seismic hazard mitigation and the nuclear test-ban treaty verification. Research is focused on topics such as lithospheric structure and intraplate seismicity.

1. INTRODUCTION

The Institute of Seismology, University of Helsinki (ISUH) is responsible for seismic monitoring in Finland. The duties of the ISUH include government regulator duties in seismic hazard mitigation and nuclear test ban treaty verification, observatory activities and operation of the Finnish National Seismic Network (FNSN) as well as research and teaching of seismology at the University of Helsinki. The FNSN (Figure 1) comprises of 31 permanent stations located throughout Finland. The FNSN is part of the Global Seismographic Network and the recordings and observational data are forwarded to several international seismic data centers (ORFEUS, ISC, EMSC, IRIS, GEOFON).

In addition to permanent stations, several denser portable networks have been established for the needs of different research interests. In 2019, a dense seismic network was installed to Helsinki in order to observe smaller seismic events in the Helsinki region. The HelsinkiNet improves the determination of locations of the events compared to the situation where only the national network is used. The network is owned by City of Helsinki and maintained by ISUH. The first stations of the HelsinkiNet were established on outer limits of Helsinki in Kuninkaantammi (KUNI), Vuosaari (VUOS), and Lauttasaari (LAUT) for maximum areal coverage. In 2021, the network was supplemented by a station in Ruskeasuo (RSUO).

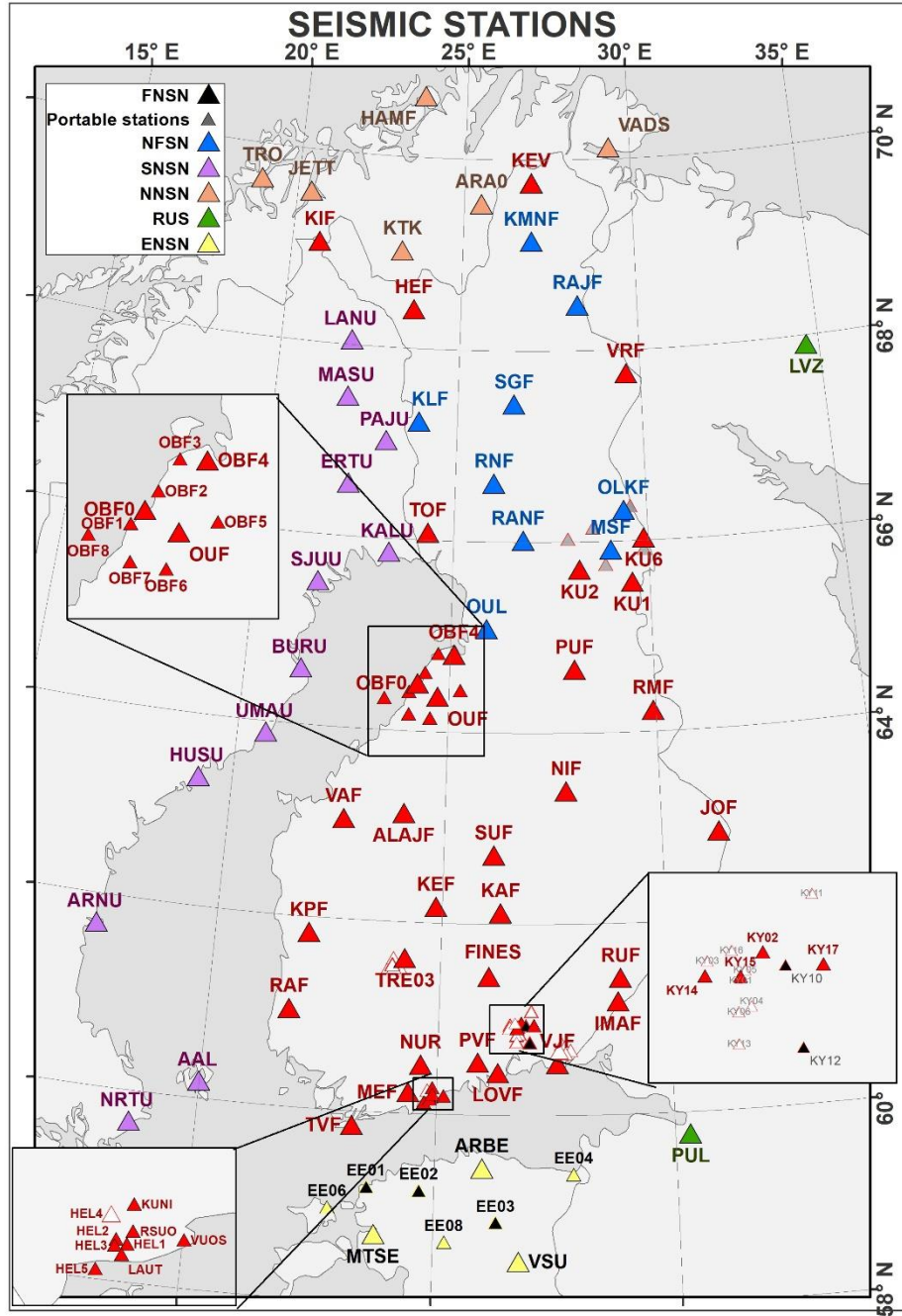


Figure 1: The Finnish National Seismic Network consists of 31 permanent seismic stations and several temporal stations. Denser networks have been installed in the areas of special interest, such as the HelsinkiNet, Kouvolan and monitoring network in Pyhäjoki.

Saaristomeren Lövskär-Isokari väylän pohjoisosan voimakkaat virtaukset

H. Kanarik¹, L. Tuomi¹, A. Westerlund¹ ja P. Alenius¹

Ilmatieteen laitos, hedi.kanarik@fmi.fi

Abstrakti

Saaristomeri on ainutlaatuinen merialue lukuisine saarineen ja luotoineen. Alueen virtausolojen tunteminen on tärkeää niin vedenvaihtotutkimusten kuin meriliikenteen turvallisuudenkin kannalta. Ilmatieteen laitos (sekä aiemmin Merentutkimuslaitos) on tehnyt lukuisia projektiluontoisia virtausmittauksia Saaristomerellä, joita on nyt kootusti tutkittu ympäristöministeriön rahoittamassa MAAMERI-projektissa. Alueen vaihtelevan geometrian ja syvyyden johdosta virtauksissa on alueellisesti suuria vaihteluita. Kapeissa ja syvissä väylissä on mitattu Itämeren olosuhteisiin nähdyn voimakkaita virtauksia. Erityisen huomiota herättävä on Lövskär-Isokari väylän pohjois-eteläsuuntainen suora, jolla on aiemmissa tutkimuksissa raportoitu erittäin voimakkaita virtauksia. Kutsumme kyseistä mittauspistettä läheisen saaren mukaan Norrgrundetiksi.

Virtaukset mitattiin Teledyne RD Instrumentsin Workhorse Sentinel 300 kHz:n ADCP:llä 1 m syvysresoluutiolla 30 minuutin jaksoissa kahtena erillisenä aikavälinä: 6.9.2016–16.10.2018 ja 20.5.–3.12.2021. Alustavat tulokset näyttävät, että voimakkaita virtauksia esiintyy alueella huomattavan usein: 5 m syvyydellä virtaukset ylittivät 30 cm/s nopeuden 15 % mittausajasta ja olivat suhteellisen pitkäkestoisia (keskimäärin 8 tuntia). Virtaukset suuntautuivat pääosin luoteeseen ja pohjoiseen eli ulos Saaristomereltä. Helmikuussa 2017 ADCP mittasi alueella 115 cm/s virtauksia voimakkailta 20 m/s kaakkoistuuilla. Tämän tapauksen aikana virtausnopeus ylitti 80 cm/s yli 6 h ajan.

The time derivative of the geomagnetic field has a short memory

M. Kellinsalmi^{1,2}, A. Viljanen¹, L. Juusola¹ and S. Käki^{1,2}

¹ Finnish Meteorological Institute, Helsinki, Finland, mirjam.kellinsalmi@fmi.fi

² University of Helsinki, Helsinki, Finland

Abstract

Space weather, eventually produced by eruptive phenomena in the Sun, can have harmful effects on high-voltage power grids via geomagnetically induced currents (GIC). GIC are a complex phenomenon, closely related to the time derivative of the geomagnetic field, $d\mathbf{B}/dt$. However, the behaviour of $d\mathbf{B}/dt$ is chaotic and has proven to be a challenge to predict. In our study, we look at the dynamics of the horizontal part of the geomagnetic field, \mathbf{H} , and its time derivative, $d\mathbf{H}/dt$, during active space weather. One of our main findings is that the direction of $d\mathbf{H}/dt$ has a very short "reset time", around two minutes, but \mathbf{H} does not show this kind of behaviour. We conclude that this result gives insight into the time scale of ionospheric current systems, which are the primary driver behind $d\mathbf{H}/dt$ behaviour.

1. INTRODUCTION

Geomagnetically induced currents (GIC) in technological conductor networks are driven by the geoelectric field. These fields are associated with the time derivative of the geomagnetic field, $d\mathbf{B}/dt$, via Faraday's induction law. This is why the time derivative, $d\mathbf{B}/dt$, can be used as a proxy for GIC (Viljanen *et al.*, (2001)). $d\mathbf{B}/dt$ is associated with "external" electric currents in the ionosphere and magnetosphere and "internal" electric currents induced in the conducting ground by rapid variations of the external part of the magnetic field. The measured geomagnetic field can be computationally divided into two parts; one that is created by currents in the ionosphere and magnetosphere (external part, \mathbf{B}_{ext}) and another that is created by the induced currents in the Earth's crust and mantle (internal part, \mathbf{B}_{int}). The rapid variations of the external current systems are a space weather phenomenon driven by solar disturbances. At auroral latitudes, the most significant external current systems are the westward electrojet, extending from pre-midnight to pre-noon local time sectors, and the eastward electrojet, extending from pre-noon to pre-midnight local time sectors.

Previous studies (e.g. Pulkkinen *et al.*, (2011), Kwagala *et al.*, (2020)) have shown that the behaviour of $d\mathbf{B}/dt$ is complex, and difficult to predict. We also know that large $d\mathbf{H}/dt$ happen mainly during westward electrojets, with southward oriented \mathbf{H} (Viljanen *et al.*, (2011)), there is a clear change in the dynamics of magnetic field fluctuations in temporal scale from 80 to 100

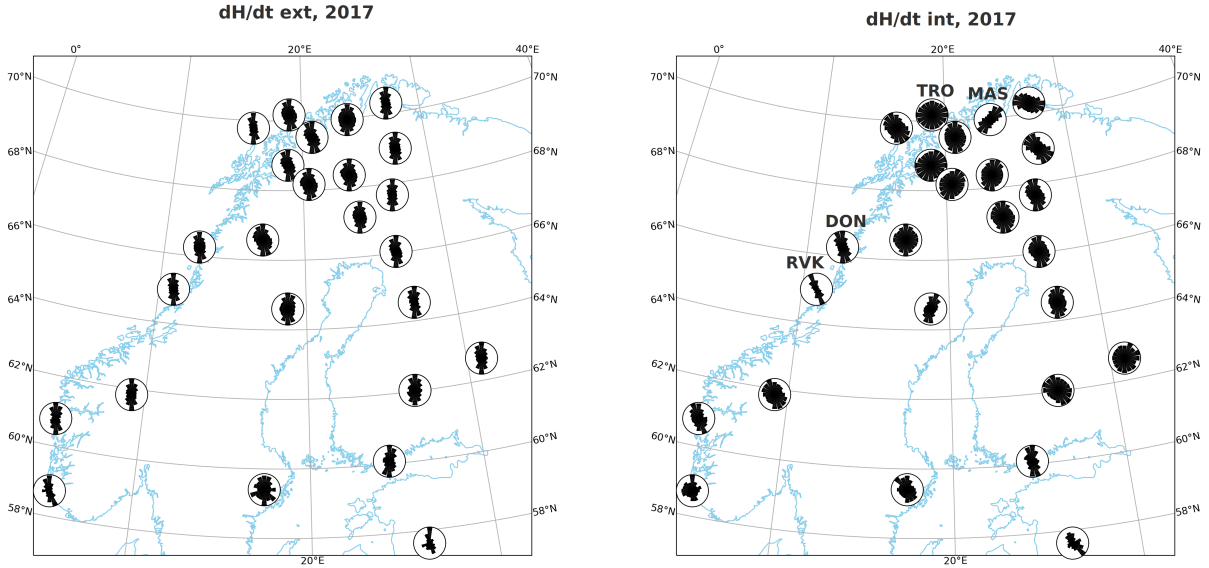


Figure 1: Directional distribution of external (left) and internal (right) $d\mathbf{H}/dt$ at IMAGE stations in 2017 when $|d\mathbf{H}/dt| > 1 \text{ nT/s}$ (*Kellinsalmi et al.*, (2022)).

s (*Pulkkinen et al.*, (2006)) and the directional distribution of the internal $d\mathbf{H}/dt$ ($d\mathbf{H}_{\text{int}}/dt$) is much more complex than that of the external $d\mathbf{H}/dt$ ($d\mathbf{H}_{\text{ext}}/dt$), due to the complex structure of the electric currents induced by the $d\mathbf{H}_{\text{ext}}/dt$ in the three-dimensional conducting ground (*Juusola et al.*, (2020)).

2. DATA AND METHODS

We use 10 s, baseline-subtracted data from the IMAGE (International Monitor for Auroral Geomagnetic Effects) magnetometer network between 1996-2018. This study is based on the separated magnetic field data. The separation was done as in *Juusola et al.*, (2020), using the 2D Spherical Elementary Current System method (SECS). We study the yearly directional distributions, and change in direction, $\Delta\theta$ (positive clockwise), of the separated horizontal geomagnetic field, \mathbf{H} , and its time derivative, $d\mathbf{H}/dt$. $\Delta\theta$ is calculated over varying time intervals, T , which is a multiple of the data sampling interval. This study is limited to active space weather conditions, defined by large values of $|d\mathbf{H}/dt|$ ($> 1 \text{ nT/s}$).

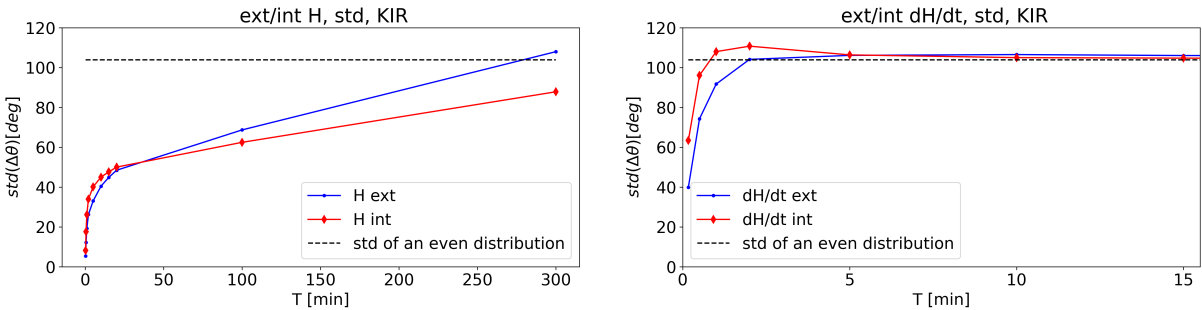


Figure 2: Standard deviations of $\Delta\theta$ for the external (blue line with dot markers) and internal (red line with diamond markers) \mathbf{H} (left panel) and $d\mathbf{H}/dt$ (right panel) as a function of T at Kiruna (KIR). Threshold value for chosen events is $|d\mathbf{H}/dt| > 1$ nT/s. Adapted from *Kellinsalmi et al.*, (2022).

3. RESULTS AND DISCUSSION

In this study we first look at the directional distributions of \mathbf{H} and $d\mathbf{H}/dt$ separately for the external and internal magnetic fields. We discovered mainly southward orientations with both \mathbf{H}_{ext} and \mathbf{H}_{int} , related to the westward ionospheric currents, north-south orientations with $d\mathbf{H}_{ext}/dt$, and more scattered orientations of $d\mathbf{H}_{int}/dt$. This backs up and extends results from previous research, e.g. *Viljanen et al.*, (2001), *Viljanen et al.*, (2011) and *Juusola et al.*, (2020).

We also notice clear, station specific differences in the directional distribution of $d\mathbf{H}_{int}/dt$. See Fig. 1 (right panel) for reference. These may be due to ground conductivity differences at the respective stations, for example, TRO in Fig. 1 has an almost even distribution, and MAS has a narrow northeast-southwest distribution. Also the coastal effect, due to a large ground conductivity gradient across the coastline (*Lilley* (2007)), is visible in the results tending to rotate \mathbf{H}_{int} perpendicular to the coastline, (see stations RVK, DON in Fig. 1). Lastly, we note that there is little variation in the directional distributions and mean directions between years. However, $d\mathbf{H}_{int}/dt$ has more scattered distributions than $d\mathbf{H}_{ext}/dt$. The yearly distributions are not shown here.

In the last part of our analysis we studied the directional change of \mathbf{H} (Fig. 2 left panel) and $d\mathbf{H}/dt$ (Fig. 2 right panel) over varying time periods, T , their $\Delta\theta$, and its standard deviation. The main new result discovered in this analysis is the asymptotic value, of about $104-110^\circ$, for $\Delta\theta(d\mathbf{H}/dt)$ standard deviation. This is approximately the value for the standard deviation of an even distribution. It was reached at about $T = 2$ min, and holds true for the external, internal and total $d\mathbf{H}/dt$ (see Fig. 2 for reference). This time scale is similar as in *Pulkkinen et al.*, (2006), although it is found using an entirely different method. However, $\Delta\theta(\mathbf{H})$ did not reach such asymptotic value. We understand this so that the direction of $d\mathbf{H}/dt$ is not predictable based on the previous values. In other words, the time derivative of the geomagnetic field quickly "loses" its memory.

4. CONCLUSIONS

The results regarding the asymptotic value for $std(\Delta\theta)$ of $d\mathbf{H}/dt$ give insight into the time scale of ionospheric current systems, which are the primary driver behind the time derivative's behaviour. It also emphasises a very short persistence of $d\mathbf{H}/dt$ compared to \mathbf{H} . Lastly, the result highlights the challenges in predicting $d\mathbf{H}/dt$ (and GIC).

5. ACKNOWLEDGEMENTS

We thank Academy of Finland for funding this project (grant no. 314670). Also, we thank the institutes that maintain the IMAGE Magnetometer Array: space.fmi.fi/image.

LÄHTEET

- Juusola, L., H. Vanhamäki, A. Viljanen, and M. Smirnov, 2020. Induced currents due to 3D ground conductivity play a major role in the interpretation of geomagnetic variations *Annales Geophysicae*, **38**, 983-998.
- Kellinsalmi, M., A. Viljanen, L. Juusola, and S. Käki, 2022. The time derivative of the geomagnetic field has a short memory, *Ann. Geophys. Discuss.* [preprint], <https://doi.org/10.5194/angeo-2022-4>, in review, 2022.
- Kwagalal, N., M. Hesse, T. Moretto, P. Tenfjord, C. Norgren, G. Toth, T. Gombosi, H.M. Kolstø, and S. Spinnangr, S., 2020. Validating the Space Weather Modeling Framework (SWMF) for applications in northern Europe: Ground magnetic perturbation validation *Journal of Space Weather and Space Climate*, **10**.
- Lilley, T., 2007, COAST EFFECT OF INDUCED CURRENTS, *Encyclopedia of Geomagnetism and Paleomagnetism*, D. Gubbins and E. Herrero-Bervera, Eds. Dordrecht: Springer Netherlands, 61–65.
- Pulkkinen, A., A. Klimas, D. Vassiliadis, V. Uritsky and E. Tanskanen, 2006, Spatiotemporal scaling properties of the ground geomagnetic field variations, *J. Geophys. Res.*, **111**, no. A3, p. A03305, doi: 10.1029/2005JA011294.
- Pulkkinen, A., M. Kuznetsova, A. Ridley, J. Raeder, A. Vapirev, D. Weimer, R.S. Weigel, M. Wiltberger, G. Millward, L. Rastätter, M. Hesse, H.J. Singer, and A. Chulaki, 2011. Geospace Environment Modeling 2008–2009 Challenge: Ground magnetic field perturbations. *Space Weather*, **9**.
- Viljanen, A., H. Nevanlinna, K. Pajunpää, and A. Pulkkinen, 2001. Time derivative of the horizontal geomagnetic field as an activity indicator *Annales Geophysicae*, **19**, 1107-1118.
- Viljanen, A. and E. Tanskanen, 2011. Climatology of rapid geomagnetic variations at high latitudes over two solar cycles *Annales Geophysicae*, **29**, 1783-1792.

Geofysiikka louhintavauriotutkimuksissa

R. Kiuru¹, L. Jacobsson², D. Király³ ja J. Suikkanen⁴

¹ Oy Rock Physics Finland Ltd, Vantaa

² RISE Research Institutes of Sweden, Borås, Ruotsi

³ SOM System Kft, Budapest, Unkari

⁴ Posiva Oy, Olkiluoto

Abstract

Excavation damage, specifically its extent and effects on hydraulic conductivity, is one of the key factors when assessing the long-term safety of deep geological disposal of spent nuclear fuel (Mustonen et al. 2010). Posiva Oy has contracted a wide variety of research related to excavation damage, among which geophysics has played a key role especially since 2008. This research includes, among other topics, geophysical measurements in tunnels and drillholes, as well as a comprehensive suite of geophysical laboratory tests. Posiva's state-of-the-art understanding of excavation damage, observing it, and its effects was recently published as a POSIVA-report (Follin et al. 2021) and as Posiva Working Reports (Kiuru et al. 2019, Heikkinen et al. 2022, Kiuru, 2019, Kovács et al. 2019, Jacobsson et al. 2019) that act as a foundation for the POSIVA-report. This presentation focuses on geophysical laboratory testing (Kiuru et al. 2019) and geophysical tests done in the research site ONK-TKU-3620 (Heikkinen et al. 2022).

TIVISTELMÄ

Louhintavaario, erityisesti sen laajuus ja vaikutus kallion vedenjohtavuuteen, on yksi käytetyn ydinpoltoaineen pitkäaikaisturvallisuutta arvioitaessa tarkasteltavista avaintekijöistä (Mustonen et al. 2010). Posiva Oy on teettänyt laajoja louhintavaurioon liittyviä tutkimuksia, joissa geofysiikka on ollut avainasemassa etenkin vuodesta 2008 lähtien. Näihin tutkimuksiin liittyen on tehty geofysikaalisia mittauksia tunneleissa ja rei'issä, sekä kattava valikoima geofysikaalisia laboratoriomittauksia. Posivan ajantasaisin käsitys louhintavauriosta, sen havainnoinnista sekä vaikutuksista on äskettäin julkaistu POSIVA-raporttina (Follin et al. 2021) sekä POSIVA-raporttia pohjustavina työraportteina (Kiuru et al. 2019, Heikkinen et al. 2022, Kiuru, 2019, Kovács et al. 2019, Jacobsson et al. 2019), joissa kuhunkin aihepiiriin mennään syvemmälle. Tämä esitys keskittyy geofysikaaliin laboratoriomittauksiin (Kiuru et al. 2019) sekä tutkimuskupriksassa ONK-TKU-3620 suoritettuihin geofysikaaliin mittauksiin (Heikkinen et al. 2022).

VASTUUVAPAUSSLAUSEKE JA ETURISTIRIIDAT

Esitetyt näkemykset ja mielipiteet ovat tekijöiden, eivätkä ne välittämättä vastaa Posiva Oy:n kantaa. Tämä tutkimus perustuu Posiva Oy:n rahoittamaan työhön.

LÄHDELUETTELO

Follin, S., L. Koskinen, J. Suikkanen, N. Riihilauma, P. Kantia, R. Kiuru ja S. Mustonen, 2021. *Characterisation of EDZ for Final Disposal Facility of Spent Nuclear Fuel in Olkiluoto*. POSIVA Report 2021-16. Posiva Oy, Olkiluoto.

Heikkinen, E., P. Kantia, R. Kiuru ja N. Riihilauma, 2022. *EDZ Study Area in ONK-TKU-3620: Geophysical Tests Conducted Between 2012 and 2014*. Posiva Working Report 2017-53. Posiva Oy, Olkiluoto.

Kiuru, R., E. Heikkinen, D. Kovács ja L. Jacobsson, 2019. *EDZ Study Area in ONK-TKU-3620: Petrophysical, rock mechanics and petrographic testing and analysis conducted in drill core specimens between 2014 and 2016*. Posiva Working Report 2017-56. Posiva Oy, Olkiluoto.

Kiuru, R., 2019. *EDZ Study Area in ONK-TKU-3620: Association Analysis of Petrophysical and Rock Mechanics Data*. Posiva Working Report 2016-42. Posiva Oy, Olkiluoto.

Kovács, D., G.M. Dabi, T. Toth, L. Jacobsson ja R. Kiuru, 2019. *EDZ Study Area in ONK-TKU-3620: Discrete Fracture Network Based Modelling of Microcrack System in Drill Core Specimens and Comparisons with Petrophysical Measurements*. Posiva Working Report 2016-56. Posiva Oy, Olkiluoto.

Jacobsson, L., G. Kjell, L. Brander ja R. Kiuru, 2019. *EDZ Study Area in ONK-TKU-3620: Determination of Seismic Wave Velocities at Six Load Levels, Petrophysical and Rock Mechanical Properties of Drill Core Specimens*. Posiva Working Report 2016-57. Posiva Oy, Olkiluoto.

Mustonen, S., J. Norokallio, S. Mellanen, T. Lehtimäki ja E. Heikkinen, 2010. *EDZ09 Project and Related EDZ Studies in ONKALO 2008-2010*. Posiva Working Report 2010-27. Posiva Oy, Olkiluoto.

Troposphere Characterization with Space Geodetic Techniques

Vicky Liu¹, Maaria Nordman^{1,2} and Nataliya Zubko²

¹ School of Engineering, Aalto University, vicky.liu@aalto.fi

² Finnish Geospatial Research Institute (FGI), National Land Survey of Finland

Abstract

The troposphere contains a massive amount of water vapor, and most weather phenomena occur in this layer. The effect of the troposphere in space geodetic techniques, such as Very Long Baseline Interferometry (VLBI) and Global Navigation Satellite System (GNSS), appears as an extra delay in the measurement of the electromagnetic signals traveling from distant radio sources (such as quasars) or satellites to the receiver. The tropospheric delay is one of the major error sources in VLBI and GNSS analysis. In this study, we investigated the agreement of the VLBI and GNSS tropospheric Zenith Wet Delay (ZWD) and examined the seasonal variability of the ZWD time series from VLBI and GNSS for eight globally distributed co-located sites with the period of eight years (Jan. 2012–Dec. 2019). The seasonal model was applied for investigating the residual ZWD as well as for determining the amplitude and trend. The ZWD time series show clear seasonal variations for all co-located sites. The VLBI ZWD is in good agreement with GNSS; this is proved by high correlation coefficients, varying from 0.72 to 0.94 for VLBI vs. GNSS. The residual ZWD were reduced significantly after removing seasonal terms from the ZWD time series. As expected, the tropical region site presented the largest amplitude compared to the temperate and polar regions. The seasonal mean of the ZWD reflects the seasonal water vapor content variability in different climate regions. The ZWD data analysis shows that the tropical region experiences high humidity during the summer and much less rainfall during the winter. The polar region is characterized by relatively low humidity with a small difference between the summer and winter seasons.

Seismisyyttä Viipurin rapakivialueella

T. Luhta¹, K. Komminaho¹ ja P. Mäntyniemi¹

¹ Seismologian instituutti, Helsingin yliopisto, tuija.luhta@helsinki.fi

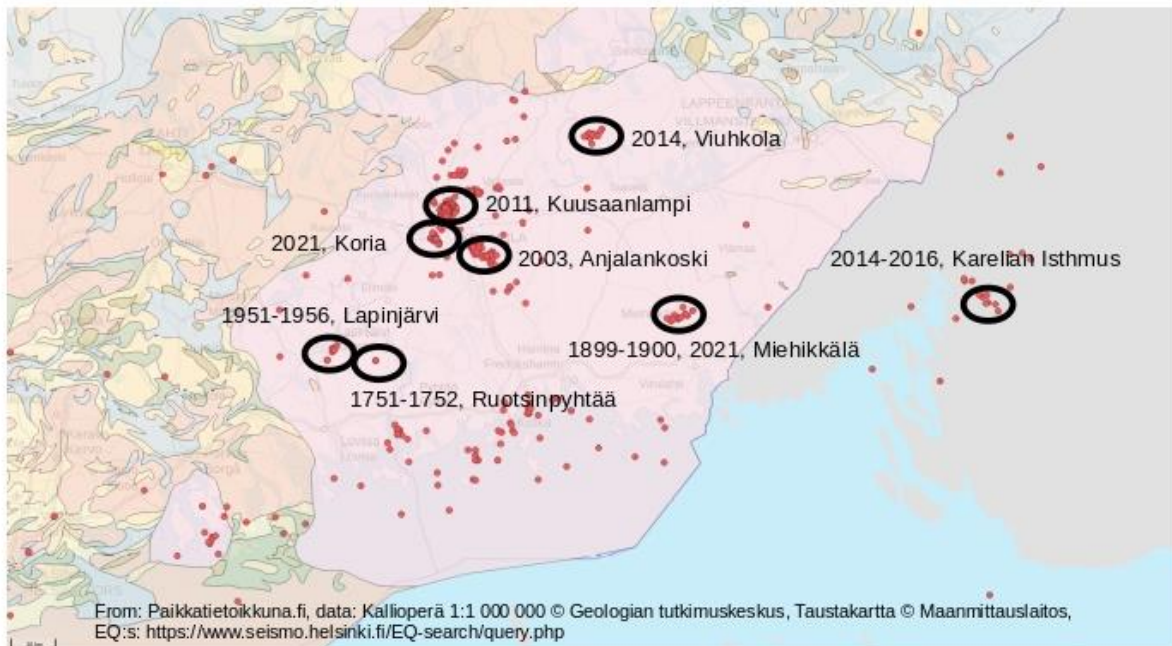
Abstract

We discuss earthquake data available for the Vyborg rapakivi granite batholith in south-eastern Finland. A specific feature of rapakivi seismicity is prolonged earthquake sequences, or swarms, but single earthquakes occur as well. Pre-instrumental earthquake sequences are known from the municipality of Ruotsinpyhtää in 1751, Miehikkälä in 1899-1900 and Lapinjärvi in the early 1950s. They are taken to be of seismic origin because of similarity to instrumental occurrences. The Lapinjärvi sequence was the longest and strongest so far, causing some non-structural damage to masonry structures. A dense network of instruments was deployed in the batholith after an earthquake sequence began close to Kuusaanlampi on the 1st of December 2011, resulting in hundreds of micro-earthquakes registered in the area. Other recent swarms occurred in Viuhkola in 2014, in the vicinity of Vyborg in 2014-2016 and in Miehikkälä and Koria in 2021. Investigations of instrumental data have shown that seismicity is confined to the uppermost 1-3 km of the crust. The shallow focal depths explain why the events are widely observed by local residents despite the small magnitudes, typically far below local magnitude M_{L3} .

1. JOHDANTO

Viipurin rapakivialue on ympäröivää kallioperää kevyempää ja nuorempaa ainesta, 1.6–1.3 Ga vanhaa (esim. Elo ja Korja, 1993). Se erottuu ympäristöstään myös seismisyyden perusteella, sillä siellä havaitaan toisinaan useiden maanjäristysten parvia (kuva 1), jotka kestävät kutakuinkin samoilla paikoilla jopa useita kuukausia. Rapakivialueella sattuu myös yksittäisiä maanjäristyksiä ja muutaman järistyksen ryppäätiä. Tiheän mittausverkon ansiosta alue on näkynyt järistysten lukumäärän perusteella keskeisenä Suomen seismisyyalueena 2010-luvulla.

Rapakivialueen järistykset tapahtuvat tyypillisesti hyvin lähellä maanpintaa, 1–2 kilometrin syvyydessä. Tästä syystä alueen järistykset herättävät usein paljon paikallista huomiota ja niistä saadaan lukuisia kansalaishavaintoja, vaikka järistykset eivät olisi kovin suuria (esim. Uski et al. 2006). Matalan syvyyden vuoksi rapakivialueen pienet järistysten erottaminen räjäytyksistä on haastavaa (esim. Saari, 1998).



Kuva 1: Viipurin rapakivialueelta tunnetut maanjäristykset toukokuuhun 2022 asti. Järistysten episentrit on merkitty punaisilla palloilla. Merkittävimmät järistysparvet on korostettu mustilla soikioilla. Suomen puolen rapakivialueet näkyvät kartassa vaaleanpunaisena.

2. HISTORIALLISIA (EI-INSTRUMENTAALISIA) TIETOJA

Laiteaikaa edeltäviltäkin vuosisadoilta on säilynyt merkintöjä maanjäristysten kaltaisista ilmiöistä Viipurin rapakivialueella. Varhaisin tunnetaan maininta maanliikkeestä raapustettiin tilikirjan marginaaliin Valkealassa 1610 (Renqvist, 1930). Ruotsinpyhtäältä raportoitiin useamman kuukauden kestävää maantärähtelyä ja pauketta loppuvuodesta 1751 ja Miehikkälästä 1899–1900. Niitä pidetään alkuperältään seismisinä etupäässä samankaltaisuuden perusteella, koska rapakivialueella on sattunut pitkittyneitä järistysparvia myös mittauslaitteiden aikakaudella (Uski et al., 2006). Talven aikana havaitut tärinät ja paukkeet voivat olla myös routajäristyksiä, joita havaitaan pitkin maata (esim. Kejonen, 2012).

Huomattava järistysparvi alkoi Lapinjärvellä elokuussa 1951 ja jatkui melkein yhtäjaksoisena seuraavan vuoden huhtikuulle (kuva 2). Voimakkaimmat tapaukset aiheuttivat joidenkin rakennusten muuratuille osille ei-rakenteellista haittaa. Ilman laitehavaintoja tapausten voimakkuuden arviointi jäi epätarkaksi, mutta vertailu viimeaisiin järistyksiin viittaa siihen, että ainakin magnitudi 3 ylittyi.

Silloisen Hydrografisen toimiston tutkijat Allan Sirén ja Nils Koroleff tekivät kentämatkan Lapinjärvelle maaliskuussa 1952. He keräsivät paikallisten asukkaiden havaintoja erityisellä kyselylomakkeella. Ajoitus ei ollut kaikkein onnekkain, sillä tutkijoiden ollessa paikan päällä mitään poikkeuksellista ei sattunut, mutta siihen asti voimakkaimmat järistykset sattuivat heidän juuri palattuaan Helsinkiin (Mäntyniemi, 2017). Kentämatkan mahdollisti Geofysiikan Seuran myöntämä avustus.

**Tarinää, helinää ja rappausten
putoilua Lapinjärvellä toissa yönä**

**Tähänastisista voimakkaimmat
maan tärähtelyt – kuultiin 16 kmn pähän**

Kuva 2: *Helsingin Sanomien* uutisointia Lapinjärven maanjäristyksistä 19. maaliskuuta 1952.

3. MITTAUSLAITTEIDEN TUOMAA TIETOA

Suomessa on rekisteröity paikallisia maanjäristyksiä ja muita seismisiä tapauksia 1950-luvulta alkaen, mutta vasta 2000-luvulla asemaverkko on rakennettu niin tiheäksi, että hyvin pienetkin järistykset voidaan havaita. Suomen kansallisen seismisen verkon havaintokynnys koko maassa on ylimmillään magnitudin 1 ja useimmilla alueilla merkittävästi matalampi (Kortström et al., 2018).

Viipurin rapakivialueelta ei ole merkitty Suomen maanjäristysluetteloon Lapinjärven tapausten jälkeen 1900-luvulta kuin joukko pieniä, suurin osa alle magnitudin yksi, maanjäristyksiä Lovisan seudulla 1980-luvulla. Ne saatiin rekisteröityä Lovisan ydinvoimalan lähialueen seimisyyttä kartoittavan paikallisen asemaverkon ansiosta (Saari, 1998). Ensimmäinen mittauslaitteiden tallentama rapakivialueen maanjäristysparvi alkoi Anjalankoskella toukokuussa 2003 ja kesti kolme viikkoa. Tapaiksista suurimman magnitudi oli 2,1. Järistykset tunnettiin laajalti. Paikalliset raportoivat ikkunoiden ja lasien helinää sekä räjähdyksen tai ukkosen tapaisia äänihavaintoja (Uski et al., 2006).

Muutamia yksittäisiä tapauksia lukuun ottamatta Viipurin rapakivialue oli seismisesti hyvin hiljainen seuraavat kahdeksan vuotta kunnes joulukuussa 2011 Kuusaanlammella alkoi uusi järistysparvi, joka osoittautui pitkäkestoiseksi. Ensimmäisen, suurimman järistyksen magnitudi oli 2,8. Se tunnettiin kymmenien kilometrien päässä. Monet luulivat tapausta suureksi räjähdykseksi ja siitä tuli lukuisia ilmoituksia pelastuslaitokselle. Sittemmin Kouvolan alueella on havaittu satoja järistyksiä. Valtaosa on hyvin pieniä, mutta kymmenet ovat olleet ainakin lähipien asukkaiden havaitsevia ja muutamasta suurimmasta on tullut hälytyksiä pelastuslaitokselle. Hälytysten syynä eivät ole olleet vahingot maanjäristyksen aiheuttamat vahingot, vaan järistyksiä on toistuvasti epäilty räjäytyksiksi.

Seismologian instituutti asensi ensimmäiset tutkimusasemat Kouvolan alueelle heti joulukuun 2011 järistyksen jälkeen. Verkon tiheys on vaihdellut sen perustamisen jälkeen muutamasta asemasta kymmeniin. Tiheimillään se oli heinäkuusta 2020 toukokuuhun 2021, jolloin toteutettiin Kuusaanlampi-verkko. Siihen kuului parhaimmillaan noin viisikymmentä geofonija kahdeksan laajakaistaseismometriä. Verkon mittaustuloksista saadaan tarkat lähdeparametrit mittausaikana tapahtuneille järistyksille. Tarkoitus on myös tutkia seismisen aallon nopeutta ja siinä tapahtuneita muutoksia verkon alueella. Nopeuskenttä kertoo kallioperän rakenteesta ja pohjaveden liikkeistä. Seismologian instituutti jatkaa mittauksia Viipurin rapakivialueella.

Lähivuosina tavoitteina on seismisyyden laajempi seuranta koko alueella sekä tihennetyn verkon asentaminen Kotkaan.

Kouvolan alueen lisäksi Viipurin rapakivialueella on havaittu 2000-luvulla järistysparvet mm. Viuhkolassa, Viipurin lähellä ja viimeimmäksi vuonna 2021 sekä Korialla että Miehikkälässä (kuva 1). Rapakivialueelle tyypillisiä matalia järistyksiä on tapahtunut myös Etelä-Suomen pienempien rapakivialueiden yhteydessä, merkittäväimpänä vuonna 2021 Ahvenanmaan rapakivialueella havaitut neljä järistystä, jotka olivat suurimmat siellä mittaushistorian aikana havaitut seismiset tapaukset.

4. YHTEENVETO

Viipurin rapakivialueella ilmenee vilkasta järistystoimintaa, josta on kirjattuja havaintoja 1600-luvulta alkaen. Mittauslaitteiden verkko on rakennettu riittävän tiheäksi 2000-luvulla, jotta pieniä maanpinnan lähellä sattuvia maanjäristyksiä voidaan tutkia monipuolisesti. Pienestä koostaan huolimatta rapakivialueen järistykset ovat aiheuttaneet paljon huomiota ja jopa huolta erityisesti niihin liittyvien räjähdysten kaltaisten äänten vuoksi.

Aiempaa tarkemman ja jatkuvasti karttuvan havaintoaineiston ansiosta voidaan tutkia järistyksiä mahdollisesti laukaisevia ympäristötekijöitä sekä kallioperän rakennetta rapakivialueella. Perusteellisempi alueen seismisyyden kartoitus tuo myös lisääaineistoa seismisen hasardin määrittelyyn alueella.

LÄHTEET

- Elo, S. ja A. Korja, 1993. Geophysical interpretation of the crustal and upper-mantle structure in the Wiborg rapakivi granite area, southeastern Finland. *Precambrian Res.*, **64**, 273-288.
- Kejonen, A., 2012. Routajäristyksistä ja niiden aiheuttamista routahalkeamista. *Geologi*, **64**, 47-50.
- Kortström, J., M. Uski ja K. Oinonen, 2018. The Finnish National Seismic Network, Summary of the Bulletin of the International Seismological Centre, 52 (I):41–52. <https://doi.org/10.31905/JSWEM8MG>
- Mäntyniemi, P., 2017. Macroseismology in Finland from the 1730s to the 2000s. Part 2: From an obligation of the elite to citizen science. *Geophysica*, **52**, 23-41.
- Renqvist, H., 1930. Finlands jordskalv. *Fennia*, **54**, 1-113.
- Saari, J., 1998. Regional and local seismotectonic characteristics of the area surrounding the Loviisa nuclear power plant in SE Finland. Helsingin yliopiston Seismologian instituutin S-raportti 36.
- Uski, M., T. Tiira, A. Korja ja S. Elo, 2006. The 2003 earthquake swarm in Anjalankoski, south-eastern Finland. *Tectonophysics*, **422**, 55-69.

3-D modelling of the geoelectric field in Fennoscandia with laterally nonuniform and plane wave inducing sources

E. Marshalko¹, A. Viljanen¹, M. Kruglyakov², and A. Kuvshinov³

¹ Finnish Meteorological Institute, Helsinki, Finland, elena.marshalko@fmi.fi

² University of Otago, Dunedin, New Zealand

³ Institute of Geophysics, ETH Zürich, Zürich, Switzerland

Abstract

In this study, we carry out three-dimensional ground electric field (GEF) modelling in Fennoscandia with the use of laterally nonuniform and plane wave inducing sources for three days of the Halloween geomagnetic storm: 29-31 October 2003. We then calculate geomagnetically induced currents (GIC) based on the obtained GEF and compare modelling results with GIC observations at the Mäntsälä pipeline recording point. Higher correlation with measured GIC is observed for GIC modelled with the use of the plane wave source, which may indicate the shortcomings of our nonuniform source construction method.

1. INTRODUCTION

Geomagnetic field disturbances caused by such space weather events as coronal mass ejections and high-speed streams in the solar wind generate so-called geomagnetically induced currents (GIC) in electric power grids and in oil and gas pipelines, which may pose a significant risk to the reliability and durability of such infrastructure. The core task in quantitative estimation of the hazard to technological systems from space weather is as realistic as practicable numerical modelling of GIC. The critical component of such modelling is the simulation of the ground electric field (GEF), which depends on the electrical conductivity distribution inside the Earth and the spatiotemporal structure of geomagnetic field fluctuations.

The most common and widely used approach to the GEF modelling is the plane wave method, where the primary electromagnetic (EM) field is represented by a vertically propagating plane wave (Pirjola, 1982). Usually, the conductivity distribution in the Earth is assumed to be one-dimensional, either uniform or vertically stratified. Recent advancements in the development of three-dimensional (3-D) EM modelling codes allow us to take into account effects in the GEF arising from 3-D conductivity structures as well as effects arising from lateral nonuniformity of the external current (the source of the EM induction).

In this work, we perform 3-D GEF modelling for three days of the Halloween geomagnetic storm: 29-31 October 2003. It is one of the most famous and well-studied geomagnetic storms on record. During this event, the Malmö region in southern Sweden experienced a large-scale

blackout caused by GIC (Pulkkinen et al., 2005). We carry out GEF modelling using a 3-D conductivity model of Fennoscandia, SMAP (Korja et al., 2002), and different models of the inducing source: a laterally nonuniform ionospheric equivalent current and a vertically propagating plane wave. The availability of GIC data recorded at the Mäntsälä pipeline GIC measurement point allows us to compare GIC calculated based on the simulated GEF with observations.

2. METHODOLOGY

In this work, for the GEF calculation we employ the real-time 3-D electric field modelling method recently developed by Kruglyakov et al. (2022). This allows us to significantly reduce the computational load compared to our standard modelling approach described, for example, in Marshalko et al. (2021), without loss of accuracy. The method relies on the factorisation of the source by spatial modes and time series of respective expansion coefficients and exploits precomputed GEF kernels generated by corresponding spatial modes. A realistic source is built using the Spherical Elementary Current Systems method as applied to magnetic field data from the IMAGE network of observations. The factorisation of the recovered source is then performed using the principal component analysis. The GEF kernels are precomputed using the PGIEM2G 3-D EM modelling code (Kruglyakov and Kuvshinov, 2018).

Another method that we employ for the GEF calculation is the "plane wave" method with the use of so-called intersite magnetotelluric impedances that relate the surface horizontal electric field at a predefined number of sites with the surface horizontal magnetic field at a fixed base site (see, e.g., Marshalko et al. (2020) for more information). In this study, the base site is the Nurmijärvi geomagnetic observatory. Magnetic field data recorded at this observatory are used for the GEF calculation using the plane wave method. The intersite impedances at the Mäntsälä GIC pipeline recording point are calculated based on the results of 3-D EM forward modelling using the PGIEM2G code with two (laterally uniform) plane wave sources.

GIC at the Mäntsälä pipeline recording point are calculated based on the GEF data in the following way: $\text{GIC}(t) = aE_x(t) + bE_y(t)$, where coefficients a and b depend only on the topology and resistances of the pipeline system. In this study, we use parameters determined by Pulkkinen et al. (2001): $a = -70 \text{ A}\cdot\text{km/V}$ and $b = 88 \text{ A}\cdot\text{km/V}$. It should be noted that above expression is a simplification and it assumes that the GEF over the pipeline area is spatially uniform.

3. MODELLING RESULTS

A snapshot of the GEF magnitude and direction in the Fennoscandian region simulated using the real-time modelling technique is demonstrated in Figure 1. According to our results, this is one of the moments of the peak amplification of the GEF in the region, which occurred at 20:03:30 UT, 30 October 2003. According to the Malmö blackout timeline presented by Pulkkinen et al. (2005), at 20:03:43 UT, 400/130 kV transformer caused overload in the 130 kV network.

Results of GIC calculation demonstrate high correlation with observations. The correlation coefficient between observed GIC and GIC modelled with the use of a laterally nonuniform inducing source is 0.7729. The correlation coefficient between observed GIC and GIC modelled with the use of a plane wave source is 0.9171. However, the values of the modelled GIC appear

Figure 1: A snapshot of the magnitude and direction of the horizontal GEF in Fennoscandia at 20:03:30 UT, 30 October 2003, simulated using the real-time modelling technique. Locations of the Nurmijärvi geomagnetic observatory (NUR), Mäntsälä pipeline GIC recording point, and Malmö city centre are marked with circles. Solid black lines mark the main branches of the Finnish gas pipeline (in 2003). Dashed black line marks the pipeline continuing to Russia.

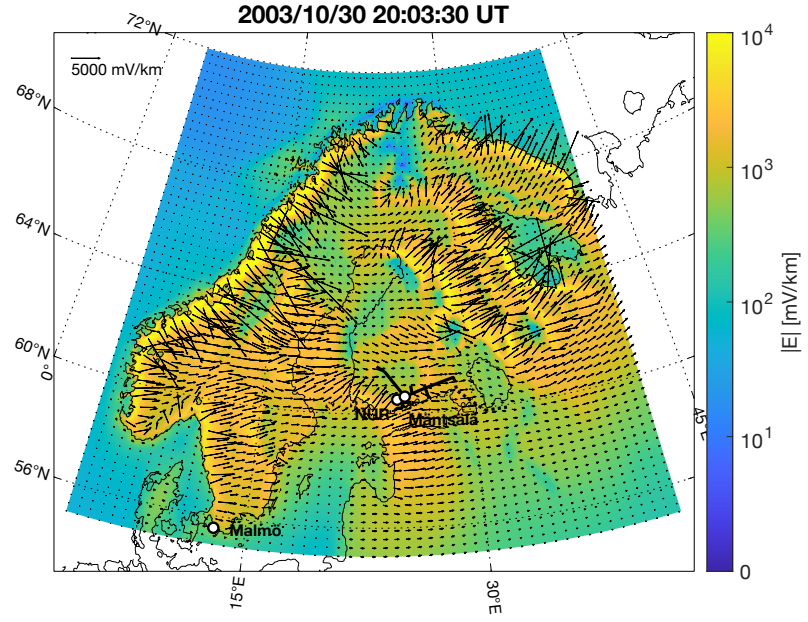
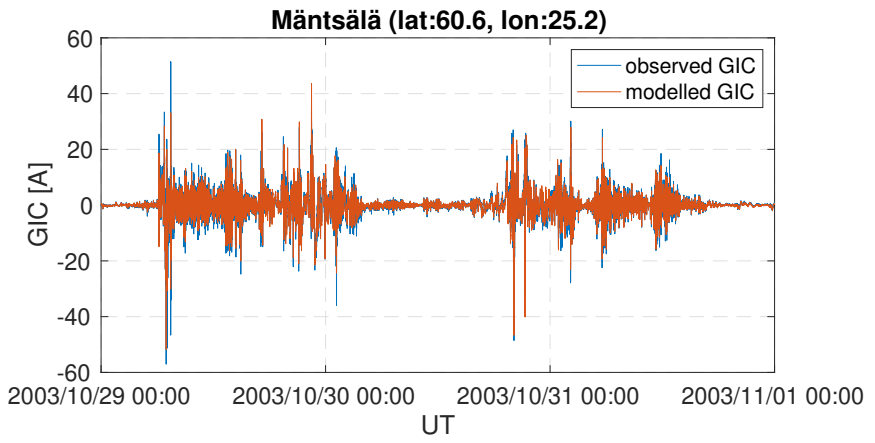


Figure 2: Time series of GIC observed at the Mäntsälä pipeline recording point and GIC calculated at the same location using Pulkkinen et al. (2001) parameters and scaled electric field modelled using the plane wave approximation.



to be largely overestimated and have to be scaled by a factor of 4.94 (laterally nonuniform source) and 5.77 (plane wave) to fit the measured GIC. In Figure 2, observed GIC are compared with GIC calculated using Pulkkinen et al. (2001) parameters and scaled electric field modelled using the plane wave approximation.

4. CONCLUSIONS

High correlation between modelled and measured GIC is observed both in case of modelling with the use of laterally nonuniform and plane wave inducing sources. The correlation between observed GIC and GIC modelled with the use of plane wave source is significantly higher than the correlation coefficient between observed GIC and GIC modelled with the use of a laterally nonuniform inducing source. This may indicate shortcomings of the external equivalent current construction process leading to the loss of accuracy.

Another conclusion is that GIC modelled with the use of both types of the source appear to be largely overestimated compared with observed GIC. In the study of Dimmock et al. (2019), GIC calculated at the Mäntsälä pipeline recording point based on Pulkkinen et al. (2001) parameters and GEF simulated in the SMAP conductivity model were also scaled by a factor of 4. This indicates that the crustal resistivity in this part of the SMAP model is most likely too high, which also leads to unrealistic conductivity contrasts contributing to the amplification of the electric field.

ACKNOWLEDGEMENTS

This work has been supported by the Academy of Finland grants no. 314670 (EM, AV) and no. 339329 (AV). MK has been supported by the New Zealand Ministry of Business, Innovation & Employment through Endeavour Fund Research Programme contract UOOX2002. AK has been supported in the framework of Swarm DISC activities, funded by ESA contract no. 4000109587, with the support from EO Science for Society. We thank the institutes that maintain the IMAGE Magnetometer Array. GIC recordings were performed in collaboration with Gasum Oy.

REFERENCES

- Dimmock et al., 2019. The GIC and geomagnetic response over Fennoscandia to the 7–8 September 2017 geomagnetic storm. *Space Weather*, **17**(7), 989–1010.
- Korja et al., 2002. Crustal conductivity in Fennoscandia – a compilation of a database on crustal conductance in the Fennoscandian Shield. *Earth, Planets and Space*, **54**, 535–558.
- Kruglyakov, M. and Kuvshinov, A., 2018. Using high-order polynomial basis in 3-D EM forward modeling based on volume integral equation method. *Geophysical Journal International*, **213**(2), 1387–1401.
- Kruglyakov et al., 2022. Real-time 3-D modeling of the ground electric field due to space weather events. A concept and its validation. *Space Weather*, **20**, e2021SW002906.
- Marshalko et al., 2020. Exploring the influence of lateral conductivity contrasts on the storm time behavior of the ground electric field in the eastern United States. *Space Weather*, **18**(3), e2019SW002216.
- Marshalko et al., 2021. Comparing three approaches to the inducing source setting for the ground electromagnetic field modeling due to space weather events. *Space Weather*, **19**(2), e2020SW002657.
- Pirjola, R., 1982. Electromagnetic induction in the Earth by a plane wave or by fields of line currents harmonic in time and space. *Geophysica*, **18**(1–2), 1–161.
- Pulkkinen et al., 2001. Recordings and occurrence of geomagnetically induced currents in the Finnish natural gas pipeline network. *Journal of Applied Geophysics*, **48**(4), 219–231.
- Pulkkinen et al., 2005. Geomagnetic storm of 29–31 October 2003: Geomagnetically induced currents and their relation to problems in the Swedish high-voltage power transmission system. *Space Weather*, **3**(8), S08C03.

Merenpinnan nousu Suomessa: historiallinen trendi ja uusimmat ennusteet

H. Pellikka¹, M. Johansson², M. Nordman^{1,3} ja K. Ruosteenoja²

¹ Rakennetun ympäristön laitos, Aalto-yliopisto, havu.pellikka@aalto.fi

² Ilmatieteen laitos

³ Paikkatietokeskus, Maanmittauslaitos

Abstract

We examine future sea level rise in Finland in light of IPCC's Sixth Assessment Report (AR6) and other published projections. Unlike previous IPCC reports, AR6 projections cover the full range of potential future sea level rise, including the "low probability, high impact" tail of the distribution. Projections for the Finnish coast by 2100 are presented. In addition, we calculate trends of absolute regional sea level rise from Finnish tide gauge data over 1901–2018. These trends are in accordance with global mean rates.

1. JOHDANTO

Todennäköisyysjakaumina esitetyt merenpinnan nousuennusteet ovat tärkeitä mm. rannikon maankäytön ja rakentamisen suunnittelussa, sillä erilaisissa kohteissa täytyy varautua eritasoihin riskeihin. Esimerkiksi tavallisen asuintalon, sairaalan ja ydinvoimalan kohdalla riskinsietokyky on erilainen. Merenpinnan nousuennusteissa on kuitenkin suurta epävarmuutta etenkin todennäköisyysjakauman yläpäässä eli korkeissa ennusteissa, joiden toteutumisen todennäköisyys on pieni. Epävarmuudet liittyvät merellisten mannerjäätiköiden, ennen kaikkea Länsi-Antarktiksen, epävakauseen lämpenevässä ilmastossa.

Hallitustenvälinen ilmastonmuutospaneeli IPCC julkaisi kuudennessa arvointiraportissaan (IPCC, 2021) uudet ennusteet merenpinnan noususta. IPCC:n aiempia ennusteita on kritisoitu liiasta konservatiivisuudesta ja todennäköisyysjakauman yläpään huomiotta jättämisestä (Hinkel et al. 2015). Kirjallisuudessa on säännonmukaisesti esiintynyt IPCC:n ylärajoja korkeampia ennusteita (Garner et al. 2018). Kuudennessa raportissa IPCC antaa ensimmäistä kertaa paikalliset ennusteet, jotka ottavat huomioon myös jakauman yläpään. Raportti antaa lisäksi erikseen matalamman luotettavuuden (*low confidence*) ennusteen, jossa on huomioitu huonosti tunnettuja ja vielä kiistanalaisia mannerjäätiköiden epävakausmekanismeja.

Suomessa merenpinnan taso on historiallisesti laskenut suhteessa maahan voimakkaan maankohoamisen vuoksi. Aikaisemmin suhteellisen merenpinnan tason trendistä oli vaikea erottaa merenpinnan nousun ja maankohoamisen keskinäisiä osuuksia, mutta geodeettisten mittausten ja mallien kehityessä on tullut mahdolliseksi arvioida maankohoamista vedenkorkeushavain-

noista riippumattomasti. Tällöin voidaan laskea absoluuttisen merenpinnan nousun nopeus. Tarkastelemme tässä työssä näitä trendejä mareografihavaintojen pohjalta sekä tulevaisuuden ennusteita IPCC:n kuudennen raportin ja muun kirjallisuuden valossa.

2. MENETELMÄT

Merenpinnan tason muutoksen voidaan ajatella Suomessa olevan kolmen ilmiön summa: globaali merenpinnan nousu, maankohoaminen ja tuuli-ilmoston muutoksesta johtuva Itämeren kokonaisvesimääärän muutos. Länsituulten voimistuminen nostaa merenpintaa Suomen rannikolla, koska länsivirtauiset työntävät vettä Tanskan salmien läpi ja painavat sitä Itämeren itäosiin. Johansson et al. (2014) osoittivat, että vedenkorkeuden havaitut vuosikesiarvot voidaan rekonstruoida varsin hyvällä tarkkuudella laskemalla näiden komponenttien summa:

$$h_m(i, t) = r(i, t, t_0) - d(i)(t - t_0) + w(i, t) + RO \quad (1)$$

missä h_m on merenpinnan keskimääriäinen suhteellinen korkeus paikassa i ajankohtana t , r on alueellinen absoluuttinen merenpinnan nousu suhteessa vertailuvuoteen t_0 , d on maankohoamisvauhti, w kuvailee tuuli-ilmoston muutoksen vaikutusta ja RO on vakio, jolla merenpinnan taso voidaan muuntaa kansalliseen N2000-korkeusjärjestelmään.

Mareografien mittaanasta keskimerenpinnan tasosta (h_m) voidaan laskea paikallinen absoluuttisen merenpinnan nousun r trendi, kun tunnetaan kaikki muut kaavan 1 tekijät. Tulevaa merenpinnan tasoa voidaan puolestaan tarkastella kolmen satunnaismuuttujan (r , d , w) summana, kun kaikista kolmesta komponentista on muodostettu todennäköisyysjakaumat. Tässä työssä on käytetty NKG2016LU-mallin maankohoamisarvoja (Vestøl et al. 2019). Tuuli-ilmoston muutosta on arvioitu laskemalla geostrofisen tuulen itä–länsisuuntainen komponentti Tanskan salmissa historiallisesta havaintoaineistosta ja CMIP5-ilmostomallien tuloksista. Merenpinnan nousua on tarkasteltu sovittamalla todennäköisyysjakaumia joukkoon kirjallisuudesta poimittuja merenpinnan nousuennusteita ja huomioimalla alueelliset poikkeamat, kuten jäätiköiden sulamisen aiheuttaman merenpinnan nousun epätasainen jakautuminen. Menetelmän yksityiskohdat on kuvattu tekeillä olevassa käsikirjoituksessa (Pellikka et al. 2022).

3. TULOKSET

Taulukossa 1 on esitetty suhteellisen merenpinnan tason sekä sen kolmen komponentin trendit muutamalla eri paikkakunnalla koko mittaushistorian ajalta sekä vuodesta 1993 vuoteen 2018.

Taulukko 1. Suhteellisen keskimerenpinnan tason (h_m), maankohoamisen (d), absoluuttisen merenpinnan nousun (r) ja tuuli-ilmostoon liittyvä merenpinnan tason muutoksen (w) trendejä Helsingissä, Turussa ja Vaasassa (mm/a).

	Vuodet	\dot{h}_m	d	\dot{w}	\dot{r}
Helsinki	1901–2018	-1.88 ± 0.19	-3.69 ± 0.18	0.49 ± 0.19	1.32 ± 0.08
Turku	1922–2018	-3.56 ± 0.24	-5.41 ± 0.17	0.59 ± 0.25	1.29 ± 0.11
Vaasa	1922–2018	-6.97 ± 0.25	-8.79 ± 0.16	0.60 ± 0.25	1.23 ± 0.11
Helsinki	1993–2018	-0.37 ± 1.89	-3.69 ± 0.18	0.17 ± 2.11	3.15 ± 0.85
Turku	1993–2018	-2.07 ± 1.81	-5.41 ± 0.17	0.16 ± 2.01	3.18 ± 0.80
Vaasa	1993–2018	-5.10 ± 1.87	-8.79 ± 0.16	0.16 ± 2.02	3.54 ± 0.76

Taulukko 2. Ennuste keskimerenpinnan tasosta eri todennäköisyystasoilla (todennäköisyysjakauman prosenttipisteet) vuonna 2100 suhteessa vuosien 1995–2014 tasoon (cm).

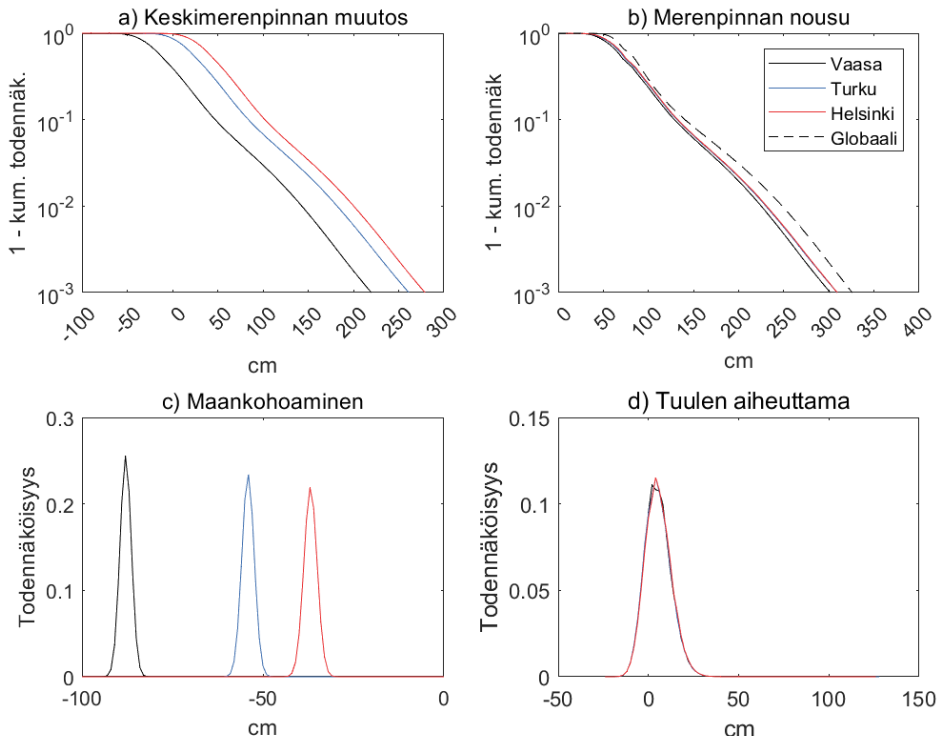
	5 %	50 %	95 %	99 %
<i>Matala päästöskenaario (RCP2.6/SSP1-2.6)</i>				
Helsinki	-22	3	42	68
Turku	-40	-15	25	51
Vaasa	-76	-51	-9	17
<i>Keskitason päästöskenaario (RCP4.5/SSP2-4.5)</i>				
Helsinki	-10	19	71	109
Turku	-28	1	53	91
Vaasa	-64	-35	17	55
<i>Korkea päästöskenaario (RCP8.5/SSP5-8.5)</i>				
Helsinki	8	46	132	200
Turku	-10	27	114	182
Vaasa	-47	-9	77	143

Ennusteet keskimerenpinnan tasosta vuonna 2100 on annettu taulukossa 2. Kuvassa 1 on esitetty eri suureitten todennäköisyysjakaumat, joista ennuste on laskettu. Merenpinnan nousun jakauma (kuva 1b) on muodostettu kymmenen eri merenpinnan nousuennusteen painotettuna yhdistelmänä, jossa on annettu suurempi paino (4) IPCC AR6:n ennusteelle (*medium confidence*) ja matalampi paino (0,5) niille ennusteille, jotka sisältävät kiistanalaisia mallituloksia mannerjäätköiden hajoamismekanismeista. Muut ennusteet ovat saaneet painokertoimen 1.

4. JOHTOPÄÄTÖKSET

Absoluuttisen merenpinnan nousun keskimääräinen nopeus on 1900-luvun alusta ollut Suomessa noin 1,2–1,3 mm/a, vuodesta 1993 noin 3,2–3,5 mm/a (taulukko 1). Eri paikkakunnille lasketut trendit ovat virherajojen puitteissa samansuuruisia eivätkä poikkeaa myöskään globaalista merenpinnan nousunopeudesta (IPCC, 2021). Tulevaisuudessa merenpinnan nousun odotetaan kuitenkin jäävän Suomessa hieman globaalialla keskiarvoa matalammaksi myös ilman maankohoamisen vaikutusta (kuva 1b). Tämä johtuu siitä, että pohjoisten jäätköiden kuten Grönlanin sulaminen ei Suomessa nostaa merenpintaa yhtä paljon kuin globaalisti.

Taulukossa 2 esitetty merenpinnan nousuennusteet poikkeavat IPCC:n kuudennen raportin ennusteista (*medium confidence*) olennaisesti lähinnä korkeassa päästöskenaariossa jakauman yläpäässä. Tämä johtuu siitä, että mukaan on otettu jäättökömallinnuksia, joista ei ole vielä tieteellistä konsensusta. IPCC on jättänyt nämä varsinaisen ennusteen ulkopuolelle, mutta antanut erikseen matalan luotettavuuden (*low confidence*) ennusteen. Kun otetaan huomioon, että korkean päästöskenaarion toteutuminen vaikuttaa solmittujen ilmastosopimusten valossa epätodennäköiseltä, voidaan sanoa, että IPCC:n keskimääräisen luotettavuuden (*medium confidence*) ennusteet soveltuvat käytettäviksi suunnittelussa, jossa voidaan sietää jonkin verran riskiä. Kohteissa, joissa riskinsierto on vähäinen, on syytä huomioida myös IPCC:n matalan luotettavuuden ennuste. Kaiken kaikkiaan IPCC:n kuudes rapportti on onnistunut aiempaa paremmin kattamaan tutkimuskirjallisuudessa esiintyvän vaihtelun merenpinnan nousuennusteissa, myös epätodennäköiset kehityskulut.



Kuva 1. Keskimerenpinnan tason (a) ja siihen vaikuttavien tekijöiden (b, c, d) todennäköisyysjakaumat vuodelle 2100 verrattuna vuosien 1995–2014 tasoon korkeassa päästöskenaariossa (SSP5-8.5/RCP8.5). Vertailun vuoksi globaalil merenpinnan nousun jakauma on piirretty katkoviivalla kuvaan b.

LÄHTEET

- Garner, A.J., J.L. Weiss, A. Parris, R.E. Kopp, R.M. Horton, J.T. Overpeck ja B.P. Horton, 2018. Evolution of 21st century sea level rise projections, *Earth's Future*, **6**, 1603–1615.
- Hinkel, J., C. Jaeger, R.J. Nicholls, J. Lowe, O. Renn ja S. Peijun, 2015. Sea-level rise scenarios and coastal risk management, *Nat. Clim. Change*, **5**, 188–190.
- IPCC, 2021. *Climate Change 2021: The Physical Science Basis. Contribution of Working Group I to the Sixth Assessment Report of the Intergovernmental Panel on Climate Change* (toim. Masson-Delmotte, V., et al.), Cambridge University Press, in press.
- Johansson, M.M., H. Pellikka, K.K. Kahma ja K. Ruosteenaja, 2014. Global sea level rise scenarios adapted to the Finnish coast, *J. Mar. Syst.*, **129**, 35–46.
- Pellikka, H., M.M. Johansson, M. Nordman ja K. Ruosteenaja, 2022. Probabilistic projections and past trends of sea level rise in Finland, *manuscript in preparation*.
- Vestøl, O., J. Ågren, H. Steffen, H. Kierulf ja L. Tarasov, 2019. NKG2016LU – A new land uplift model for Fennoscandia and the Baltic Region, *J. Geod.*, **93**, 1759–1779.

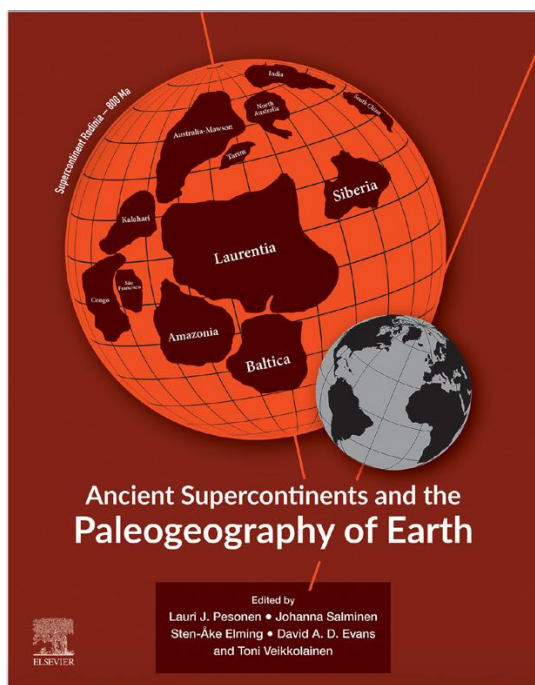
Ancient Supercontinents and the Paleogeography of Earth

L.J. Pesonen¹ and J. Salminen^{2,3}

¹ Department of Physics, University of Helsinki, FI-00014 University of Helsinki, Finland,
lauri.pesonen@helsinki.fi

² Department of Geosciences and Geography, University of Helsinki, FI-00014 University of
Helsinki, Finland

³ Geophysical Solutions, Geological Survey of Finland, Espoo, Finland



The assembly, configuration and breakup phases of supercontinents have been research topics of wide interest particularly with respect to mantle dynamics, tectonic evolution of the continents and oceans, growth of the atmosphere and cryosphere, changes in surface environment, and questions related to the origin and extinction of life forms. Supercontinent cycle on Earth has been going on since the Paleoproterozoic times (≤ 2.0 Ga) and has been the main tectonic regime involving all five spheres of our planet: geosphere, cryosphere, hydrosphere, biosphere and atmosphere. Evidence from the supercontinent cycle during Precambrian times arises from multiple observations in geoscientific disciplines such as geology, geochronology, geophysics and geochemistry. The results are also viewed in the framework of recent theoretical results provided by models of the core, mantle and lithosphere.

A consensus has appeared among the geoscience community that after the existence of supercratons during the Neoarchean-Paleoproterozoic times, the Earth has witnessed three eras of supercontinents or huge landmasses: the Paleo-Mesoproterozoic Nuna, the Meso-Neoproterozoic Rodinia and the Neoproterozoic/Phanerozoic Gondwana/Pangea assemblies, which together define the supercontinent cycle. The results suggest that the three supercontinents Nuna, Rodinia and Pangea are different and that the tectonic processes driving the supercontinent cycle are interactive involving the lithosphere, mantle and the core. Here we describe the output of a new Elsevier-published book (2021) on Precambrian supercontinents and their cyclicity.

The **scopes** of the book and its 18 Chapters, co-authored by internationally recognized geoscientists, deal with:

- (i) to define the drift histories of the major Precambrian continents, their cratonic nuclei and their building blocks focusing on the last 3 billion years;
- (ii) to test the credibilities of previously proposed Precambrian supercontinent models, to propose alternative ones, and to study their assembly, tenure and breakup phases in order to define the possible supercontinent cyclicity;
- (iii) to test the new supercontinent assemblies with upgraded geological, tectonic, geophysical, geochemical, and geochronological data;
- (iv) to investigate if the proposed supercontinent models and their cyclicity match various temporal features (peaks, troughs, pulses, excursions) and cycles as derived from time series of secular evolution proxies, such as plate tectonic, kinematic, mantle depletion, biogeological, atmospheric, and environmental;
- (v) to compare the paleomagnetically constructed supercontinent models, their phases and their cyclicity, with predictions provided by mantle dynamic modelling;
- (vi) to investigate if certain properties of the Earth's magnetic field (such as the ancient field intensity) provided by geodynamo models compare with observed paleointensity data, and if so, to shed further light on the idea that the heat-transfer phenomena occurring at the core-mantle boundary can link to observations at the surface of the Earth;
- (vii) and finally, the book raises challenging questions, e.g. why do we have supercontinents, what forces are driving the continental blocks to amalgamate or to breakup, how long is the lifetime of a supercontinent, and many others.

REFERENCES

Pesonen, L.J., J.M. Salminen, S.-Å. Elming, D.A.D. Evans, and T. Veikkolainen, 2021. Ancient Supercontinents and the Paleogeography of Earth. Elsevier Co., Amsterdam, The Netherlands, 646 pp.

Metsähovi Geodetic Research Station

**M. Poutanen¹, M. Bilker-Koivula¹, J. Eskelinen¹, U. Kallio¹, N. Kareinen¹, H. Koivula¹,
J. Näränen¹, J. Peltoniemi¹, A. Raja-Halli¹, and N. Zubko¹**

¹ Finnish Geospatial Research Institute FGI, National Land Survey of Finland,
markku.poutanen@nls.fi

Abstract

Metsähovi Geodetic Research Station (MGRS) of the National Land Survey of Finland, has been undergoing a major upgrade over the past decade. When completed, MGRS will be one of the northernmost stations in the global geodetic core network of the International Association of Geodesy (IAG) with a full suite of co-located space geodetic instrumentation, gravimeters and various auxiliary equipment. We present recent developments at MGRS and introduce the instrumentation that already contributes and will contribute in the future to various IAG services. MGRS belongs also to two Finnish Research Infrastructure (FIRI) consortiums of the Academy of Finland.

1. INTRODUCTION

Astronomical and satellite observations and radio astronomy measurements have been made at Metsähovi site in Kirkkonummi since the 1960s. The area has the facilities of the University of Helsinki, Aalto University (formerly Helsinki University of Technology) and the Finnish Geospatial Research Institute FGI (formerly the Finnish Geodetic Institute). Geodetic observations started in 1978 when the first Satellite Laser Ranging (SLR) system was completed. The first continuously observing GPS receiver was connected to the global geodetic network in 1992.

In 2012, a decade-long reform began, during which all major equipment was renewed, a new SLR and geodetic radio telescope were built, and the area's infrastructure has been completely refurbished. When completed, MGRS will be one of the most modern stations in the Global Geodetic Observing System of the IAG network. It produces continuous observations on the use of IAG services and GGOS (IAG, 2022; GGOS, 2022; Metsähovi, 2022).

2. GLOBAL GEODETIC OBSERVING SYSTEM AND METSÄHOVI

The GGOS works in conjunction with IAG's 12 services, which coordinate measurements and analyses of global geodetic networks. The core stations have all the modern geodetic equipment, including Global Navigation Satellite Systems (GNSS) receivers, Satellite Laser

Ranging (SLR), Very Long Baseline Interferometer (VLBI) radio telescope, The Doppler Orbitography and Radio-positioning Integrated by Satellite instrument (DORIS), absolute and superconducting gravimeters, and local geodetic networks and facilities to connect various observing techniques.

Together, the GGOS core stations form the solid backbone for maintaining the International Terrestrial Reference Frame (ITRF), monitoring the orientation of the Earth in space, global tectonic movements, and producing information for computing precise orbits of satellites, including GNSS.

Core station observations cannot be replaced by other technologies. The stability of the stations and their long and stable series of observations are paramount. MGRS is one of about twenty GGOS core stations. Hundreds of other geodetic stations, most of them GNSS-only, form the global geodetic network which is the basis of accurate geospatial information.

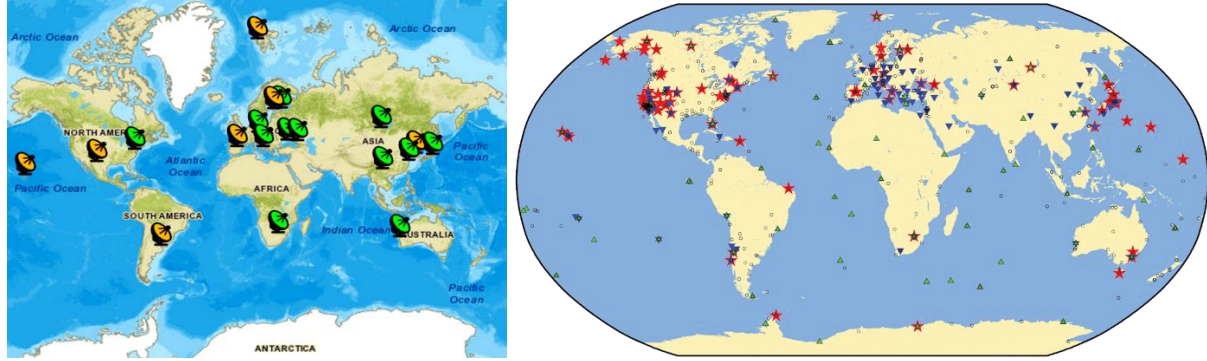


Figure 1: (Left) Core stations of the GGOS Global network. (Right) Geodetic stations defining the ITRF. Different symbols denote different techniques: GNSS (circles), VLBI (stars), SLR (blue triangles), Doris (open triangles)



Figure 2. Metsähovi Geodetic Research Station. (Photo Flux Productions)

3. INSTRUMENTATION

The MGRS currently houses several GNSS receivers, including three stations in the International GNSS Service (IGS) of the IAG network. Since 1992 MGRS has been a part of the IGS network which is the basis for maintenance of ITRF, as well as precise orbits of GNSS satellite and detailed information on crustal deformations and tectonic movements. The national reference frame is connected to the European and global frames via GNSS.

FGI started SLR observations in 1978. The current system, now in the commissioning phase, is the third one in the row. It has a modern telescope with a 0.5 m main mirror, capable to track all earth-orbiting satellites and a fast 2 kHz pulse laser and a timing system. These allow for an observing accuracy of a few millimetres in range to the low-orbit satellites, and one centimetre up to the distance of the navigation satellites. SLR activities are coordinated by the International Satellite Laser Ranging Service (ILRS) of the IAG. Globally about 40 SLR stations are tracking more than 100 active satellites with retroreflector prisms.

Geodetic VLBI observations have been made since 2004 using the radio telescope of Metsähovi Radio Observatory (MRO) of Aalto University. A few campaigns per year have been carried out. A new dedicated VLBI Global Observing System (VGOS) compatible radio telescope was built and is now in the commissioning phase. According to the VGOS specifications, there are four frequency bands in the range of 2.5 – 14 GHz. Telescopes are fast-slewing, 12-m class antennas and the system is capable of a high data rate of 8 Gbps and above. The MGRS 13.2 m telescope will be a part of the International VLBI and Astrometry Service (IVS) of the IAG.

The absolute gravimeter FG5X-221 is the national standard for the acceleration of free fall. It was upgraded in 2013. The gravimeter is operated at Metsähovi when it is not used elsewhere. It is the basis of the national gravity system and metrological comparisons with other absolute gravimeters are performed regularly. FGI has operated a superconducting gravimeter in the gravity laboratory of the MGRS since 1994, and the old instrument was replaced by two new ones in 2013-2015. The SG is capable of detecting gravity variations as small as 10^{-12} of the normal gravity. Because of its high sensitivity and very high temporal stability, the SG is eminently suitable for the study of geodynamical phenomena through their gravity signatures.



Figure 3. (Left) New SLR telescope, (middle) VLBI radio telescope, (right) local tie and telescope deformations measurement.



Figure 4. (Left) FG5X-221 absolute gravimeter, (middle) two superconducting gravimeters, and (right) DORIS beacon.

Other instruments and facilities at Metsähovi include a DORIS beacon, a trihedral triangular corner reflector for geodetic SAR measurements and calibration of TerraSAR-X observations, a local geodetic network and facilities for local tie observations between different techniques, and weather and environmental sensors. The station upgrade also includes a new office and instrumentation building that is being constructed and completed in 2022.

MGRS is a partner in the FIN-EPOS and E2S consortia, which are on the Academy of Finland (AoF) Finnish Research Infrastructure (FIRI) Roadmap. As a part of the FIN-EPOS project, funded by the AoF, a high precision time and frequency link between MGRS and the Finnish metrology institute VTT MIKES has been realized via commercial White Rabbit technology. A new optical fiber link with a capacity of 100 Gbit/s speed has been installed to support the VGOS data transfer in the future.

REFERENCES

GGOS, 2002. Global Geodetic Observing System. <https://ggos.org>

IAG, 2022. International Association of Geodesy. <https://www.iag-aig.org/>

Metsähovi, 2022. Metsähovi Geodetic Research Station.

<https://www.maanmittauslaitos.fi/en/research/research/metsahovi-geodetic-research-station>

Näränen, J., N. Zubko, J. Eskelinen, U. Kallio, A. Raja-Halli, N. Kareinen, H. Koivula, M. Poutanen, M. Bilker-Koivula, and J. Peltoniemi, 2022. Recent developments at the future GGOS core site Metsähovi, Finland. IVS General Assembly 27.3.–1.4.2022 Helsinki. Abstracts: https://www.maanmittauslaitos.fi/sites/maanmittauslaitos.fi/files/attachments/2022/03/Abstarct_book_2022.pdf

Paleomagnetic data and the Deep-time Digital Earth program

J. Salminen^{1,2}, S. Zhang³, and D.A.D. Evans⁴

¹ Geological Survey of Finland, Johanna.salminen@gtk.fi

² University of Helsinki

³ China University of Geosciences Beijing, China

⁴ Yale University, United States

Abstract

The Deep-time Digital Earth (DDE) program of the International Union of Geological Sciences (IUGS) has been developed to address the unstructured and inherently heterogeneous geoscience data that resides in institutions, universities and on individual geoscientists' computers. Under the umbrella of the DDE program, a three-year Paleomagnetism working group (<https://wg11dde.wixsite.com/website>) led by Zhang, Evans and Salminen has been established to coordinate with affiliated fields (geochronology, geophysics, paleogeography, petrology and geochemistry, stratigraphy, tectonics) in addressing both data curation and scientific integration. At present, there is still a lack of a comprehensive paleomagnetism data dictionary, knowledge system and knowledge graph that cooperate with DDE platform. The goal for the working group is to start constructing the DDE paleomagnetism knowledge graph. We also aim in establishing standards of paleomagnetic data production and existing paleomagnetic data quality criteria are proposed for evaluating the paleomagnetic data for the purpose of applications (e.g., Meert et al. 2020). In addition, the working group intent to streamline the archiving of paleomagnetic data, since deep-time paleomagnetic data are currently assembled into three global databases paleoMAGIA, MagIC (<https://earthref.org/MagIC/>), GPMDB, all of which purport to be comprehensive in scope. Two of these databases originated from the foundations of the work that has been done in the Nordic Paleomagnetic Workshops (NPW) (e.g., Brown et al. 2018). The ultimate aims of the working group, harmonization and sharing of the multidisciplinary global geoscience data and knowledge, is also a mission of DDE program.

REFERENCES

- Brown, M.C., T.H. Torsvik, and L.J. Pesonen, 2018. Nordic workshop takes on major puzzles of paleomagnetism, Eos, 99.
- Meert, J.G., A.F. Pivarunas, D.A.D. Evans, S.A. Pisarevsky, L.J. Pesonen, Z.-X. Li, S.-Å. Elming, S.R. Miller, S. Zhang, and J.M. Salminen, 2020. *Tectonophysics* **790**, 228549.

Ultra-high resolution sediment sequence from coastal Littorina sea spanning the Holocene thermal maximum – environmental magnetic study from Kurikka, Southern Ostrobothnia

S. Silvennoinen¹, J. Salminen², N. Putkinen³, and S. Kultti¹

¹ Department of Geosciences and Geography, University of Helsinki, Finland,
sonja.silvennoinen@helsinki.fi

² Geological Survey of Finland, Espoo, Finland

³ Geological Survey of Finland, Kokkola, Finland

Abstract

Both natural and anthropogenic factors cause present day hypoxia in the Baltic Sea basin (BSB), leading to the formation of sulfide sediments (Zillén et al. 2008). Moreover, acid sulfate soil is a common environmental challenge in areas of raised littoral deposits. Before present and medieval times, the BSB has experienced widespread hypoxia during the Holocene thermal maximum (HTM, ca. 8–4 ka) (Zillén et al. 2008). The extensive laminated sulfate sediments have thought to represent hypoxic conditions in the Bothnian bay throughout the early Littorina sea (Sohlenius & Öborn 2004). Yet past occurrences of BSB hypoxia have been recorded primarily in deep basin sediments cores with resolutions seldom exceeding ~0.01 cm/a. Little is still known of the seafloor redox condition variability in the littoral zone during HTM (van Helmond et al. 2017).

A promising novel proxy for oxygen depletion and redox zonation is occurrence of greigite (Fe_3S_4), a magnetic mineral that forms in sulfidic and methanogenic redox zones of the sediment-water interface (Roberts et al. 2018). Greigite has been identified from BSB sediments, (e.g. Sohlenius 1996, Kortekaas 2007, Lougheed et al. 2012, Reinholdsson et al. 2013) but the formation pathways are still under discussion.

Here, the environmental magnetic (EnvMag) methods are used to study the occurrence and characteristics of greigite in a HTM ultra-high resolution (0.75 cm/a) sediment succession from Kurikka, S. Ostrobothnia, Finland. A 40-m long sediment core was analysed for lithology, magnetic susceptibility, organic matter content, grain size and EnvMag characteristics to construct the stratigraphy and magnetic mineral composition. The sediment core covers local deglaciation, Akyllus lake and Littorina sea evolution until isolation from the sea (~10 800–4500 a).

Authigenic single-domain greigite was found from Littorina sediments with signs of sulphidic redox origin. The results propose diagenetic origin for greigite in BSB littoral sediments, contradicting the earlier suggestion - derived from deep sea environment - of bacterial-only

*origin for greigite in the BSB (Reinholdsson et al. 2013). Furthermore, unlike previous studies, no greigite was found from *Ancylus* clays. The findings indicate different greigite formation processes for the littoral zones compared to those of deep-sea basins in the BSB. This suggests that even within the same basin and sediment units, the formation pathways of greigite differ.*

*Susceptibility was coupled to EnvMag results and used to assess hypoxia variation along the sediment sequence. Hypoxia was found to be frequent although discontinuous during the HTM in the shallowing *Littorina* sea bay. The large-scale trends of hypoxia were perennial, but possibility for (sub)annual variation could not be ruled out. Two periods of centennial hypoxia were identified, while the varying greigite concentrations indicate unstable oxygen conditions. Signs of short-termed oxic conditions between low-oxygen periods (~6500–7000 cal BP) were identified. The period has been previously identified with higher salinity levels and relative sea level rise in the BSB.*

REFERENCES

- Kortekaas, M., 2007. Post-glacial history of sea-level and environmental change in the southern Baltic Sea. *LUNDQUA Thesis 57, Lund University, Department of Geology, Quaternary Sciences.*
- Lougheed, B.C., I. Snowball, M. Moros, K. Kabel, R. Muscheler, J.J. Virtasalo, and L. Wacker, 2012. Using an independent geochronology based on palaeomagnetic secular variation (PSV) and atmospheric Pb deposition to date Baltic Sea sediments and infer 14C reservoir age. *Quaternary Science Reviews*, **42**, 43-58.
- Reinholdsson, M., I. Snowball, L. Zillén, C. Lenz, and D. Conley, 2013. Magnetic enhancement of Baltic Sea sapropels by greigite magnetofossils. *Earth and planetary science letters*, **366**, 137-150.
- Roberts, A.P., X. Zhao, R.J. Harrison, D. Heslop, A.R. Muxworthy, C.J. Rowan, J.C., Larrasoña, and F. Florindo, F., 2018. Signatures of reductive magnetic mineral diagenesis from unmixing of first-order reversal curves. *Journal of Geophysical Research: Solid Earth*, **123**, 4500-4522.
- Sohlenius, G., 1996. Mineral magnetic properties of Late Weichselian-Holocene sediments from the northwestern Baltic Proper. *Boreas*, **25**, 79-88.
- Sohlenius, G., and I. Öborn, 2004. Geochemistry and partitioning of trace metals in acid sulphate soils in Sweden and Finland before and after sulphide oxidation. *Geoderma*, **122**, 167-175.
- van Helmond, N., N.B.Q. Krupinski, B.C. Lougheed, S.P. Obrochta, T. Andrén, T., and C.P. Slomp, 2017. Seasonal hypoxia was a natural feature of the coastal zone in the Little Belt, Denmark, during the past 8 ka. *Marine geology*, **387**, 45-57.
- Zillén, L., D.J. Conley, T. Andrén, E. Andrén, and S. Björck, S., 2008. Past occurrences of hypoxia in the Baltic Sea and the role of climate variability, environmental change and human impact. *Earth-Science Reviews*, **91**, 77-92.

Virolaisten maanjäristysten geologinen tulkinta

H. Soosalu^{1,2}, M. Uski³, K. Komminaho³ ja A. Veski¹

¹ Viron geologian tutkimuskeskus, heidi.soosalu@egt.ee

² Geologian instituutti, Tallinnan teknillinen yliopisto

³ Seismologian instituutti, Helsingin yliopisto

Abstract

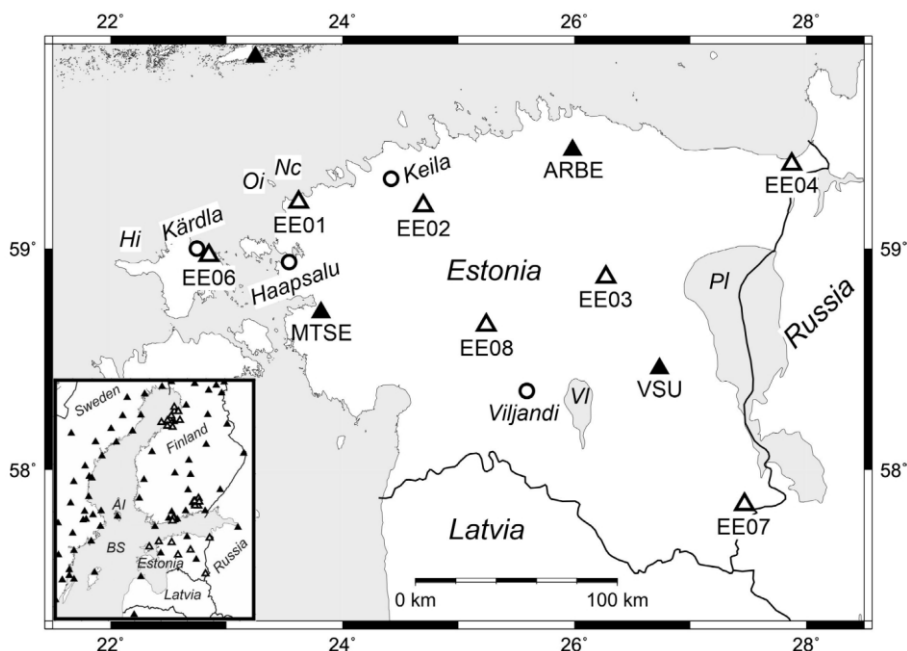
There has so far been little research of instrumentally observed earthquakes in Estonia. The Precambrian crystalline basement in Estonia is covered by a 100–600 m thick sequence of sedimentary bedrock, providing direct indications of only a few of its fault lineations. Otherwise, tectonic features of Estonian basement have been indirectly deduced from geophysical measurements, fixed with observations from drill cores. As a joint Finnish-Estonian effort, the 3-station seismic network of Estonia was augmented with seven temporary stations, providing a seismic dataset suitable for quantitative analysis. Four local earthquakes from 2016–2018 with magnitudes 1.2–2.0 were tentatively geologically interpreted. Their focal parameters were determined, and they were examined in the context of the regional stress field. The events were compared with the largest known Estonian earthquake, the magnitude-4.5 Osmussaar earthquake from 1976. Results of this analysis indicate that all these events can be associated with predominantly left-lateral strike-slip movement on NNW-SSE subvertical faults. This interpretation matches with the general stress field of northern Europe, dominated by plate movement.

1. JOHDANTO

Fennoskandian kilven laidalla sijaitsevan Viron kiteistä kallioperää peittävät n. 100–600 m paksut sedimenttikivikerrostumat ja se on Suomen tavoin seismisesti rauhallista aluetta. Maanjäristyksiä rekisteröidään keskimäärin yksi kahdessa vuodessa ja niiden magnitudit ovat harvoin kahta suurempia. Instrumentaalisia seismisiä havaintoja ja niistä tehtyjä kvantitatiivisia geologisia tulkintoja on toistaiseksi olemassa vähän.

Helsingin yliopiston Seismologian instituutti ja Viron geologian tutkimuskeskus suorittavat kansallista seismistä valvontaa yhteistyönä, käyttäen samaa analyysiohjelmistoa ja molempien maiden dataa. Yhteistyön puitteissa on viime vuosina Virossa ollut toiminnassa kolmen pysyvän seismisen aseman lisäksi Seismologian instituutin laitteistoilla varustettuna seitsemän väliaikaista asemaa mahdollistaen kohtalaisen hyvän kattavuuden (kuva 1). Vuosina 2016–2018 havaittiin eri puolilla Viroa neljä maanjäristystä magnitudivälillä 1,2–2,0. Niiden seisminen data mahdollisti analyysin, jonka olemme esitelleet tutkimuksessa Soosalu et al.

(2022), verraten niitä vuonna 1976 tapahtuneeseen 4,5-magnitudiseen ja tietävästi Viron suurimpaan Osmussaaren maanjäristykseen (esim. Slunga, 1979).

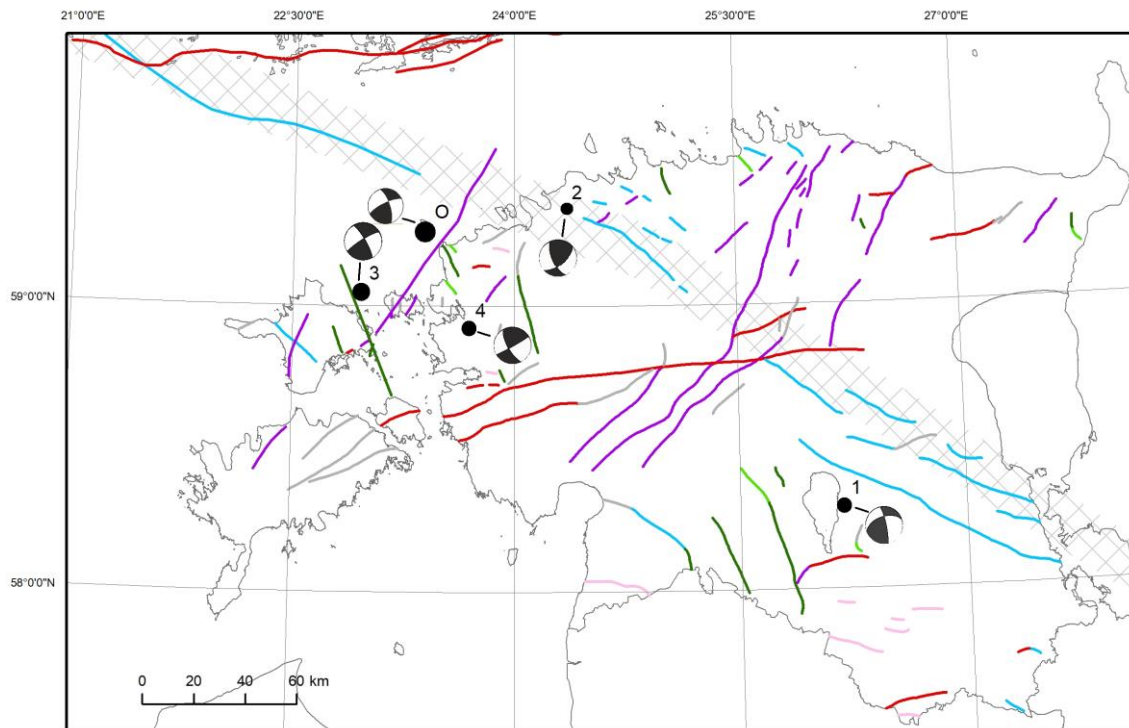


Kuva 1: Viron ja sen naapurimaiden seismiset asemaverkot, asemat on merkitty mustilla (pysyvät) ja valkoisilla (väliaikaiset) kolmioilla. Ympyröillä on merkitty maanjäristysten episentrien lähellä sijaitsevat kaupungit. Kärdla sijaitsee samannimisen meteoriittikraatterin alueella. Ål: Ahvenanmaa, BS: Itämeri, Hi: Hiumaa, Nc: Neugrundin meteoriittikraatteri, Oi: Osmussaari, P: Peipsijärvi, VI: Võrtsjärvi, julkaisusta Soosalu ym. (2022).

2. MAANJÄRISTYSAINEISTO

Tutkittujen maanjäristysten ja vertausmateriaalina käytetyn Osmussaaren järistyksen tiedot on lueteltu taulukossa 1 ja niiden sijainnit esitetty kuvassa 2. Ensimmäisen, magnitudin 1,8 tapauksen episentri sijaitsee Võrtsjärven lähistöllä, alueella, jolta on olemassa joitakin historiallisia maanjäristyshavaintoja (Doss, 1910, Nikonov ja Sildvee, 1991). Toinen, magnitudin 1,2 tapaus sattui Keilan kaupungin lähistöllä, Ahvenanmaa-Paldiski-Pihkova murrosvyöhykkeellä (ks. kuva 2). Kolmas ja suurin, magnitudin 2,0 järistys sattui merialueella Hiidenmaan saaresta koilliseen. Neljänneksi maanjäristyksen magnitudi oli 1,7 ja sen episentri on Haapsalun kaupungin alueella. Se on näistä tapauksista ainoa, josta on olemassa makroseismisia eli yleisöhavaintoja.

Hiidenmaan, Osmussaaren ja Haapsalun ympäristö on historiallisesti Viron seismisesti aktiivisinta aluetta. Sieltä on olemassa tietoja makroseismistä havainnoista 1800-luvulta alkaen. Mielenkiintoinen havainto on kahden maanjäristyksen ja meteoriittikraatterien sijaintien yhtenevyys: Osmussaaren järistyksen episentri on merenalaisen Neugrundin kraatterin tietämällä ja Hiidenmaan järistys osuu Kärdlan kraatterin reunalle. Tämänhetkisen aineiston perusteella ei voi vielä päättää, onko yhteys todellinen vai näennäinen.



Kuva 2: Viron kallioperän siirrokset väritettynä sen mukaan, mikä on niiden suuntaus Fennoskandian maksimaalisen horisontaalisen jännityksen suhteen (σH 115–135°, Korja ja Kosonen, 2015). Oletetun liikkeen suunnan ja σH :n erotus: sininen – 0°, normaalisiirros; violetti – 90°, käänteissiirros; vihreä – 30–40°, vasenkäytinen sivuttaissiirros; punainen – 30–40°, oikeakäytinen sivuttaissiirros; harmaa – muu. Maanjäristysten episentrit on merkitty mustilla palloilla, siirrostasoratkaisuja kuvaavat fokaalipallot ovat hieman niistä sivussa. Ahvenanmaa-Paldiski-Pihkova murrosvyöhyke on väritetty rasterilla. Kartta on julkaisusta Soosalu ym. (2022).

Taulukko 1: Osmussaaren 1976 maanjäristyksen* ja tutkittujen järistysten lähdeparametrit. Tapaukset (T): O – Osmussaari, 1 – Võrtsjärvi, 2 – Keila, 3 – Hiiumaa, 4 – Haapsalu. H: syvyys, F – syvyys lukittu. M: magnitudo, Osmussaari – momenttimagnitudo Mw (Korja ym., 2019), muut: paikallinen magnitudo ML Seismologian instituutin skaalan mukaan. S1, D1, R1, S2, D2, R2: kahden siirrostasovaihtoehdon kulun, kaateen ja liu'un suunnat. SA: Maksimaalisen horisontaalisen kokoonpuristumisjännityksen suunta. Muokattu julkaisun Soosalu ym. (2022) taulukosta Table 2.

T	Pvm, aika (UTC)	Lat (°N), Lon (°E)	H (km)	M	S1 (°)	D1 (°)	R1 (°)	S2 (°)	D2 (°)	R2 (°)	SA (°)
O	19761025 08:39	59.26, 23.39	10.0F	4.5	341	69	17	245	74	158	114
1	20161112 02:49	58.289, 26.187	4.0F	1.8	348	80	39	251	52	168	114
2	20170322 03:00	59.342, 24.356	4.0F	1.2	155	66	33	50	61	152	102
3	20170715 08:01	59.048, 22.961	11.4	2.0	330	79	10	238	80	168	104
4	20180304 01:21	58.925, 23.692	3.5	1.7	151	70	4	60	87	160	107

*Siirrosmekanismi: Slunga (1979), muut lähdeparametrit maanjäristyskatalogista Fencat (2020) ja siinä viitatuista lähteistä.

3. MAANJÄRISTYSTEN ANALYYSI JA GEOLOGINEN TULKINTA

Paikansimme maanjäristykset käyttäen Helsingin yliopiston Seismologian instituutissa laadittua maankuoren mallia. Tämä on Viron osalta perusteltua, koska kiteinen kallioperä on siellä samaa jatkumoa. Määrittelimme paikantamiemme maanjäristysten pitkittäis- ja poikittaisaaltohavaintojen perusteella niille hyposentrisyydet ja siirrostasoratkaisut (taulukko 1). Sekä suuren Osmussaaren maanjäristyksen että tutkittujen maanjäristysten siirrostasoratkaisut (kuva 2) ja syvyydet ovat varsin yhteneväisiä. Ne kaikki sattuivat maankuoren yläosassa, n. 4–11 km:n syvyydellä.

Kaikkien tapausten osalta ovat mahdollisia liikkeen suuntaa likimain vasenkätilinen pohjoisluode-eteläkaakko tai oikeakätilinen länsilounas-itäkoillinen. Viron kallioperän murroslinjojen perusteella pidämme todennäköisempänä vaihtoehtona vasenkätilä pohjoisluode-eteläkaakkosuuntaista siirrostumista.

Koska tutkittujen maanjäristysten magnitudit ovat kohtalaisen pieniä, on yksikäsitteisten havaintojen määrä melko rajallinen. Näin ollen voi laadittuja siirrostasoratkaisuja pitää alustavina tuloksina, jotka kuitenkin pystyy loogisesti sovittamaan vallitsevaan jännityskenttään. Tämä on olennainen alku Viron seismisyyden lainalaisuuksien selvittämiselle, jota tulevaisuuden havainnot tulevat täydentämään.

LÄHTEET

- Doss, B., 1910. Die historisch beglaubigten Einsturzbeben und seismisch-akustischen Phänomene der russischen Ostseeprovinzen. *Beitr. zur Geophysik*, **X**, 1–124.
- Fencat, 2020. Fennoscandian earthquake catalogue for 1375–2014. <https://www.seismo.helsinki.fi/bulletin/list/catalog/FENCAT.html>.
- Korja, A. ja E. Kosonen (toim.), 2015. Seismotectonic framework and seismic source area models in Fennoscandia, Northern Europe. *Inst. Seismology, Univ. Helsinki, Rep.*, **S-63**.
- Korja, A., S. Kihlman ja K. Oinonen (toim.), 2019. Seismic source areas for seismic hazard assessment in central Fennoscandia. *Inst. Seismology, Univ. Helsinki, Rep.*, **S-66**.
- Nikonov, A.A. ja H. Sildvee, 1991. Historical earthquakes in Estonia and their seismotectonic position. *Geophysica*, **27**, 79–93.
- Slunga, R., 1979. Source mechanism of a Baltic earthquake inferred from surface-wave recordings., *Bull. Seism. Soc. Am.*, **69**, 1931–1964.
- Soosalu, H., M. Uski, K. Komminaho ja A. Veski, 2022. Recent intraplate seismicity in Estonia, East European Platform. *Seismol. Res. Lett.*, **93**, 1800–1811.

Simulated sea level extremes on the Finnish coast

J. Särkkä¹, J. Räihä¹, M. Rantanen¹, and K. Jylhä¹

¹ Finnish Meteorological Institute, Jani.Sarkka@fmi.fi

Abstract

We present simulations of extreme sea levels on the Finnish coast in the Baltic Sea. These simulations can be considered as estimates of the highest sea levels that can be reached when a cyclone with strong intensity and optimal track passes the Baltic Sea region. For this purpose, sea level variations were simulated using a two-dimensional hydrodynamic model, which was forced by an ensemble of time-dependent wind and air-pressure fields taken from synthetic cyclones. We found the highest extremes on the Finnish coast in the northern Bothnian Bay and in the eastern Gulf of Finland, where the sea level maxima can be over 2.5 meters high.

1. INTRODUCTION

In the Baltic Sea, the short-term sea level variations can be several meters. The short-term sea level fluctuations are caused by passing windstorms, that induce sea level variation through wind-induced currents, inverse barometric effect and seiches. Due to the shape of the Baltic Sea with several bays, the highest sea levels are found in the ends of bays like the Gulf of Finland and the Bothnian Bay. The sea level extremes caused by the large-scale windstorms depend strongly on the storm tracks. We have studied extreme sea levels that are not found in the observation time series, having mainly less than 150 years of data.

2. METHODS AND RESULTS

To model the atmospheric conditions related to low-pressure systems, we have generated synthetic cyclones. The cyclone is modelled by describing the pressure field by a spatially varying time-dependent function that reproduces the typical cyclone characteristics. This method has been used to study sea levels in the Gulf of Finland (Averkiev and Klevannyy, 2010, Apukhtin et al., 2017), and in the Bothnian Bay (Gordeeva and Klevannyy, 2020). In our method for generating synthetic cyclones, the mean sea level pressure and surface winds of the cyclone are calculated from the pressure field of the cyclone propagating with a constant velocity. The pressure field of the cyclone has the form of a Gaussian function. Wind field is calculated from the pressure field from geostrophic balance and making some corrections to obtain surface winds

Figure 1: Example of synthetic cyclone and induced winds. Contours represent sea level pressure and wind barbs represent 10 m winds.

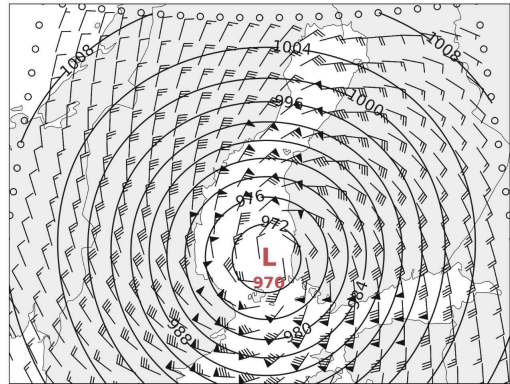


(Fig. 1). To study the variability of sea levels, induced by varying tracks of the passing windstorms, we construct an ensemble of synthetic low-pressure systems. In this ensemble, the parameters of the low-pressure systems (e.g., point of origin, velocity of the center of the system and depth of the pressure anomaly) are varied. The ensemble of low-pressure systems is used as an input to a numerical sea level model based on shallow-water hydrodynamic equations. The sea level model is fast to calculate, enabling a study of a large set of varying storm tracks. As a result, we have an ensemble of simulated sea levels. From the simulation results we can determine the low-pressure system that induces the highest sea level on a given location at the coast. Our simulation method does not include the filling of the Baltic Sea due to the water flow from the North Sea through the Danish Straits. Instead, we may add the maximum sea level rise due to the filling to the estimates by adding 1 meter to the local sea level maximum (Särkkä et al., 2017). This describes the extreme situation when preceding weather conditions have affected mean sea level and raised it high, and then the propagating low-pressure system causes fluctuations on top of the already high mean sea level. The highest simulated sea levels were found in the northern end of the Bothnian Bay and the eastern end of the Gulf of Finland, where extremes exceeding 2.5 meters are possible.

REFERENCES

- Apukhtin, A., G. Besson, S. Gordeeva, M. Klevannaya, and K. Klevannyy, 2017. Simulation of the probable maximum flood in the area of the Leningrad Nuclear Power Plant with account of wind waves, *Russian Meteorology and Hydrology*, **42**, 113–120.
- Averkiev, A.S., and K.A. Klevannyy, 2010. A case study of the impact of cyclonic trajectories on sea-level extremes in the Gulf of Finland, *Continental Shelf Research*, **30**, 707–714.
- Gordeeva, S.M., and K.A. Klevannyy, 2020. Estimation of the maximum and minimum surge levels at the Hanhikivi peninsula, Gulf of Bothnia, *Boreal Environment Research*, **25**, 51–63.
- Särkkä, J., K.K. Kahma, M. Kämäräinen, M.M. Johansson, and S. Saku, 2017. Simulated extreme sea levels at Helsinki, *Boreal Environment Research*, **22**, 299–315.

Wave-induced bottom shear stress in the coastal areas of Gulf of Bothnia

L. Tuomi¹ ja H. Kanarik¹

¹ Finnish Meteorological Institute laura.tuomi@fmi.fi

Abstract

We used third generation wave model WAVEWATCH III® (WW3) to simulate 20 years of wave condition for the Gulf of Bothnia. The accuracy of the model results was evaluated by comparing simulated values against those measured by wave buoys and satellite altimeters. According to the validation, the accuracy was good with the model slightly underestimating the significant wave height. Based on the wave-induced bottom orbital velocities calculated by WW3 and the sea bed substrate data downloaded from EMODnet Geology (www.emodnet-geology.eu) we calculated wave-induced bottom shear stress values for the Gulf of Bothnia. As expected, the results show that the effect of waves on the sediment erosion is notable only in near-coastal shallow areas. To further evaluate the wave effects on the bottom sediments we calculated how often and for how long periods the wave orbital velocities and wave-induced bottom shear stress exceeded critical values for sediment suspension to take place. The adequacy of the results is evaluated by comparing the known erosion bottoms to the model estimates.

HelsinkiNet - a collaborative seismological research network of the Institute of Seismology, and the City of Helsinki

T. Veikkolainen¹, K. Oinonen¹, T. Vuorinen¹, J. Kortström¹, P. Mäntyniemi¹, P. Lindblom¹, T. Luhta¹, J. Hällsten¹, P. Seipäjärvi¹ and T. Tiira¹

¹ Institute of Seismology, University of Helsinki, toni.veikkolainen@helsinki.fi

Abstract

This article describes the HelsinkiNet, a seismic network owned by the City of Helsinki, and maintained by the Institute of Seismology, University of Helsinki. The network was already in its test phase in 2019 capable of detecting seismic events. The full operation began in 2020 with stations in Kuninkaantammi (KUNI), Lauttasaari (LAUT), and Vuosaari (VUOS). In 2021, the network was expanded with a station in Ruskeasuo (RSUO), intended for monitoring a medium-depth heat well currently under construction. The network has registered natural earthquakes in Vantaa, and in the Gulf of Finland, close to the shore of Helsinki, Espoo, and Kirkkonummi. It has also registered induced earthquakes in Espoo, yet the vast majority of registrations are explosions. Some stations of the network were able to detect the detonation of a man-made rocket in September 2021, an event widely spread in media outlets. HelsinkiNet has its own event detector that registers signals within a 30-km distance from central Helsinki. The detector is better suited for small events near stations, than the detector of the Finnish national seismic network (FNSN), while the detector for the FNSN can better detect events elsewhere in the country and hundreds of kilometers outside it. The detector also uses other seismic stations in the Finnish capital region, leading to thousands of seismic events registered annually.

1. INTRODUCTION

Based on an initiative by the City of Helsinki, the Institute of Seismology began planning a network of three seismic stations to Helsinki in 2019. The network, named HelsinkiNet, is intended to lower the observation threshold and to improve the event detection accuracy in the built area. Its main goals are to provide scientists and authorities information on seismicity in the capital region. The use of heat wells is one of the driving forces for the project. The agreement between the city and the institute regarding the construction and the maintenance of the network was signed in August 2019, pointing out that the city owns the network and pays the institute for its service.

2. CONSTRUCTION AND ARRANGEMENT

After successful test measurements, the original network was built in 2019-2020. It consists of stations in Kuninkaantammi (KUNI), Lauttasaari (LAUT), and Vuosaari (VUOS). They are

located near the city borders to provide a favorable station geometry for events within the city area. All of them have been installed directly on the bedrock in equipment shelters. For KUNI and LAUT, the test measurement sites remained final installation sites. VUOS was relocated to Kallahdenniemi because of the high background noise at the test measurement site in eastern Vuosaari. Otherwise the noise level of HelsinkiNet stations has turned out to be low, given their urban locations. In 2021, the network was supplemented with a new station in Ruskeasuo (RSUO), established for the monitoring of the medium-depth heat well of Helen Inc. currently under construction.

The stations are part of the automatic seismic event detection systems of the Helsinki urban area, and the entire Finland (Kortström et al. 2016, Veikkolainen et al. 2021a). HelsinkiNet is also used for seismic monitoring of Finland and adjacent areas, supplementing the Finnish National Seismic Network (FNSN) in the daily data analysis. The automatic seismic event detection system of the Helsinki Urban area applies covers an area with a radius of 30 km from the Central Railway Square. A larger area would lead to a large number of misidentified events near the borders. The system is based on the software used by the national network, yet it has been tuned to better register weak signals near the stations, below the detection threshold (magnitude M0.9) of the national network. The threshold magnitude is the lowest magnitude of a seismic event completely observable anywhere in Finland.

Data delivery of the HelsinkiNet stations has also been relatively reliable without major gaps, except for KUNI where a faulty seismometer and power supply have caused occasional problems in the past. The stations have a wired connection to the electric network, although they also have batteries so that they can continue operation also during electricity outages. Under normal circumstances, the data are constantly delivered to the institute via a mobile network.

In addition to the HelsinkiNet stations, five stations (HEL1-HEL5) established by the Institute of Seismology for monitoring the St1 deep heat project have been in operation during the last few years in the western Helsinki, and Espoo during the past few years (Hillers et al. 2020). Temporary short-period seismometers have been in operation for the same purpose as well (Rintamäki et al. 2022). Because the location of seismic events improves by a favorable station geometry, data from the HelsinkiNet stations and the FNSN stations have often been supplemented with data from Estonian seismic stations for events in the Helsinki region or near the southern coast of Finland.

3. YEARLY OBSERVED SEISMIC EVENTS

The Finnish national seismic network, supplemented by HelsinkiNet stations and St1 stations, registered 2834 seismic events within the detection radius in 2019, 6755 in 2020, and 3483 in 2021. The vast majority of events were probable explosions from quarries and construction sites. Their analysis is often limited to event classification, and the automatically detected location remains the final one. Data from explosions are highly usable for developing the seismic observation system. In particular, accurate locations provided by contractors can be used to improve the location accuracy of the seismic network. For example, based on a bilateral agreement, Boskalis Terramare Inc. provided information on its marine explosions near the Vuosaari harbour to the Institute of Seismology in 2021. The strongest explosion was of M1.7 (Veikkolainen et

al. 2022).

In 2019, the construction of HelsinkiNet was underway, but seismometers could register events at test measurement sites. A natural earthquake (M0.9) was registered on the 9th of July near the Helsinki lighthouse, and a probably induced earthquake on the 9th of May at Laajalahti (Luhta et al. 2019). No other earthquakes occurred within the HelsinkiNet detection area.

In 2020, HelsinkiNet observed 24 earthquakes with $M \geq 0.0$ within its detection radius. Two of them were natural earthquakes in Hakunila, Vantaa. The first natural earthquake (M0.8) occurred on the 22th of July in the night (03:36 local time) and the second one (M0.7) on the 12th of December in the evening (21:55 local time). The institute received four citizen observations from the former, and 17 from the latter event. The events were shallow, approximately at the depth of 1 km. Most induced earthquakes took place in Otaniemi, Espoo, during the counterstimulation of St1 Inc. that lasted from the 6th to 24th of May. The strongest one of them, M1.2, was on the 16th of May, yet an equally strong event occurred before the stimulation, on the 14th of April. The respective numbers of citizen observations were 34 and 32. A few induced events ($M \leq 1.0$) also happened after the stimulation in late May and June, and in December. An induced earthquake (M1.1) was also detected in Koskelo, Espoo, on the 2nd of December, yet only one citizen observation can be related to the event (Veikkolainen et al. 2021b).

In 2021, the number of earthquakes with $M \geq 0.0$ was only six. The strongest probably induced earthquake, M1.1, occurred on the 2nd of March, and a weaker one, M0.6, on the 4th of July. Other probably induced events took place on the 27th and the 29th of December. All of them were in southeastern Espoo. These induced earthquakes support the notion that human activity may alter the local stress field in the bedrock and induce earthquakes even if no drilling operations are conducted simultaneously. Induced earthquakes may also occur in the timeframe where explosions are unlikely. The only natural earthquake registered by the HelsinkiNet during the year occurred in the sea area of Kirkkonummi on the 28th of August. The event was of M1.0 and no citizen reports are related to it due to its remote location, even though its focal depth was only about 2 km (Veikkolainen et al. 2022).

4. DETONATION IN PASILA

In the late evening of the 11th of September, 2021, the institute received citizen reports about explosive sounds and tremor from central and northern Helsinki. The automatic detection system of the institute could not register any event, but manual analysis showed a clear signal in seismograms of HelsinkiNet stations KUNI, RSUO, and VUOS, and a few other stations of the Helsinki region. Based on seismic data alone, it was possible to locate the event to northern Pasila. However, the data were submitted to Ursus Astronomical Association for a more accurate modelling and altitude estimate based on the propagation of sound waves. Results showed that the event took place at the northern edge of the railway yard of northern Pasila (60.2188° N, 24.9399° E) at an altitude of approximately 300 m. The most probable explanation for the phenomenon was an improvised explosive device. Finally, matches and other ignition equipment were found only 40 m from the calculated location. The successful chase aroused plenty of media attention.

5. FUTURE

The maintenance and development of the HelsinkiNet is governed by bilateral agreements that are renewed annually. Test measurements are being undertaken to construct a new seismic station to monitor the heat well project of the Laakso hospital.

ACKNOWLEDGEMENT

We thank Jaakko Visuri from the Ursia Astronomical Association for remarkable efforts in solving the cause for the detonation of Pasila in September 2021.

REFERENCES

- Hillers, G., T.A.T. Vuorinen, M.R. Uski, J. Kortström, P.B. Mäntyniemi, T. Tiira, P.E. Malin, and T. Saarno, 2020. The 2018 geothermal reservoir stimulation in Espoo/Helsinki, southern Finland: Seismic network anatomy and data features, *Seismological Research Letters*, **91**, 770-786.
- Kortström, J., M. Uski, and T. Tiira, 2016. Automatic classification of seismic events within a regional seismograph network, *Computers & Geosciences*, **87**, 22-30.
- Luhta, T., P. Mäntyniemi, T. Vuorinen, P. Lindblom, P. Seipäjärvi, K. Oinonen, J. Kortström, and T. Tiira, 2021b. Helsingin seisminen asemaverkko ja seismisyys 2019, *Report T-101, Institute of Seismology, University of Helsinki*.
- Rintamäki, A.E., G. Hillers, T.A.T. Vuorinen, T. Luhta, J.M. Pownall, C. Tsarsitalidou, K. Galvin, J. Keskinen, J.T. Kortström, T.-Z. Lin, P.B. Mäntyniemi, K.J. Oinonen, T.J. Oksanen, P.J. Seipäjärvi, G. Taylor, M.R. Uski, A.I. Voutilainen, and D.M. Whipp, 2021. A Seismic Network to Monitor the 2020 EGS Stimulation in the Espoo/Helsinki Area, Southern Finland. *Seismological Research Letters*, **93**, 1046-1062.
- Veikkolainen, T., J. Kortström, T. Vuorinen, I. Salmenperä, T. Luhta, P. Mäntyniemi, G. Hillers, and T. Tiira, 2021a. The Finnish National Seismic Network: Toward Fully Automated Analysis of Low-Magnitude Seismic Events, *Seismological Research Letters*, **92**, 1581-1591.
- Veikkolainen, T., K. Oinonen, T. Vuorinen, J. Kortström, P. Mäntyniemi, P. Lindblom, M. Uski, and T. Tiira, 2021b. Helsingin seisminen asemaverkko ja seismisyys 2020, *Report T-103, Institute of Seismology, University of Helsinki*.
- Veikkolainen, T., K. Oinonen, T. Vuorinen, J. Kortström, P. Mäntyniemi, P. Lindblom, T. Luhta, J. Hällsten, and T. Tiira, 2022. Helsingin seisminen asemaverkko ja seismisyys 2021, *Report T-106, Institute of Seismology, University of Helsinki*.

Extreme geomagnetic storms in Northern Europe

A. Viljanen¹, E. Marshalko¹, and I. Honkonen¹

¹ Finnish Meteorological Institute, ari.viljanen@fmi.fi

Abstract

Assessment of extreme geomagnetic variations is a scientifically interesting challenge and of high practical importance due to space weather impacts on modern infrastructure. We present a previous data-based study in Northern Europe, and results from a recent simulation of the famous geomagnetic Carrington storm in 1859. The simulation indicates that the magnetic storms observed in modern times have been clearly smaller than the Carrington event.

1. INTRODUCTION

Space weather originates from the interaction of the solar activity and solar wind with the geomagnetic field. Its visual appearance as auroral displays is spectacular, but related geomagnetic variations can have detrimental effects on modern infrastructure. A time-varying magnetic field is associated with a geoelectric field, which in turn drives currents in all conductors. Currents flowing in technological conductor systems such as high voltage power grids are called geomagnetically induced currents (GIC). In the worst case, GIC can cause long-term wide blackouts as in Québec, Canada, in March 1989 (Bolduc, 2002).

The era of modern technology vulnerable to space weather is still very short, so there is not yet experience of extreme geomagnetic storms known to have occurred in the past. A famous example is the Carrington event in 1859 (Clauer and Siscoe, 2006) when auroras were seen close to the equator. Sporadic magnetic observations of that time indicate variations much larger than observed thereafter (Blake et al., 2020).

In this presentation, a data-based estimation of extreme geomagnetic variations and the related geoelectric field in the Nordic countries is summarised. Then we compare these results to a recent simulation of the Carrington storm.

2. EXTRAPOLATIONS FROM OBSERVATIONS

Long-lasting measurements of the geomagnetic field provide a starting point for statistical estimation of extreme variations. More precisely, this can provide, for example, an assessment of how large a variation occurring once in 100 years could be. One effort was made by Myllys et al. (2014) who performed a GIC study for the Norwegian high-voltage power grid. Based on magnetometer recordings of a 18-year period (1994-2011), they modelled the geoelectric field

in Norway. As a simplification, they assumed a layered ground conductivity model across the whole region. This is appropriate for the present purpose, but full 3D induction modelling has also recently become feasible (e.g., Marshalko et al., 2021).

Figure 1 shows the maximum values of the electric field in 1994-2011 as black dots. Extrapolated values of the 100-year maximum are plotted as green dots. Roughly speaking, they are about twice the 18-year maximum. Finally, Myllys et al. (2014) considered a large magnetic storm on 13-14 July 1982, which occurred outside of the original time series. The maximum value of the modelled electric field at available observatories from Germany to Finland is plotted as blue dots in Fig. 1. At high magnetic latitudes (north Finland), the electric field is equal to the estimated 1-in-100 years value, whereas at lower latitudes the 1982 storm exceeds the 1-in-100 years event. It is also noteworthy that very large electric fields occur even at Danish latitudes.

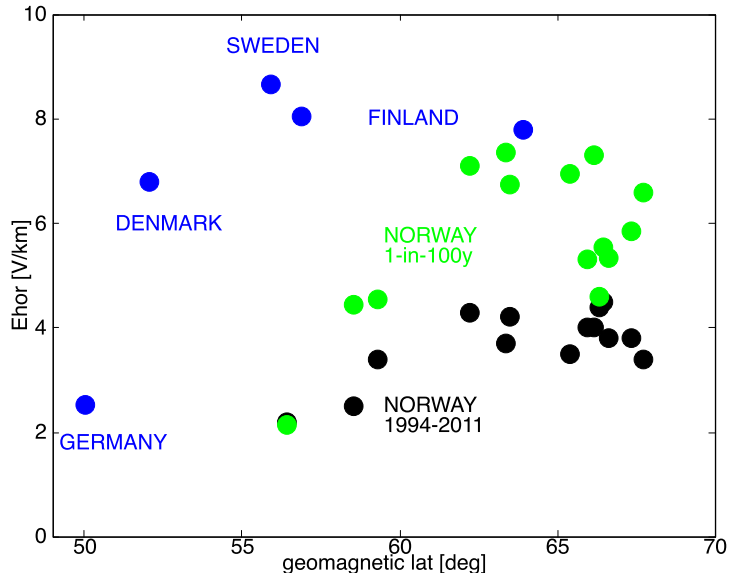


Figure 1: Maximum value of the modelled geoelectric field (horizontal component, 1-min data; Myllys et al., 2014). Black dots: values based on magnetometer recordings at Norwegian latitudes in 1994-2011. Green dots: extrapolated 1-in-100 years maximum. Blue dots: modelled maximum values based on data from geomagnetic observatories on 13-14 July 1982. The horizontal axis is the magnetic latitude. Geographic locations are indicated by country names.

3. RESULTS FROM SIMULATIONS

Due to the lack of high-resolution geomagnetic data, we cannot directly model the geoelectric field of the Carrington storm. Additionally, the relatively short coverage of modern data limits the reliability of extrapolated field variations of very rare events (1-in-100 years or less frequently). An alternative way is to apply first-principle physics to simulate the interaction between the solar wind and the geomagnetic field. Using expected extreme solar wind parameters, simulations result finally in the variations of the ground magnetic field. From this field, it is then possible to model the geoelectric field.

We discuss here briefly the simulation by Blake et al. (2021) who were able to reproduce the geomagnetic observations at Colaba, India, during the Carrington storm in 1859. The solar wind parameters were adjusted so that the deep decline of the horizontal magnetic field near the equator appeared in a very similar manner in the simulated ground magnetic field. Since the simulation covers the whole globe in a dense grid as 1-min time series, it is possible to study the behaviour of the ground magnetic field at all latitudes. Figure 2 shows the maximum of the time derivative of the horizontal magnetic field vector in the northern hemisphere. For comparison, the largest known measured value (from 1-min data; Lovö in Sweden on 13 July 1982) is indicated as a red dot. The largest simulated value is about twofold. High latitudes such as the Nordic countries are most affected similarly to the July 1982 case in Fig. 1, but remarkably large values occur down to about latitude 40° N.

We note that the simulated ground field is produced only by ionospheric and magnetospheric currents, whereas measured values also contain the contribution by induced currents in the conducting ground. This means that the simulated magnetic field, and especially its time derivative, is underestimated (cf. Juusola et al., 2020). As a side note, Blake et al. (2021) set the magnetic pole to its estimated location in 1859, from which it has changed latitudinally more than 10 degrees. So a precise comparison to the present may require rerunning the simulation with an updated magnetic pole location.

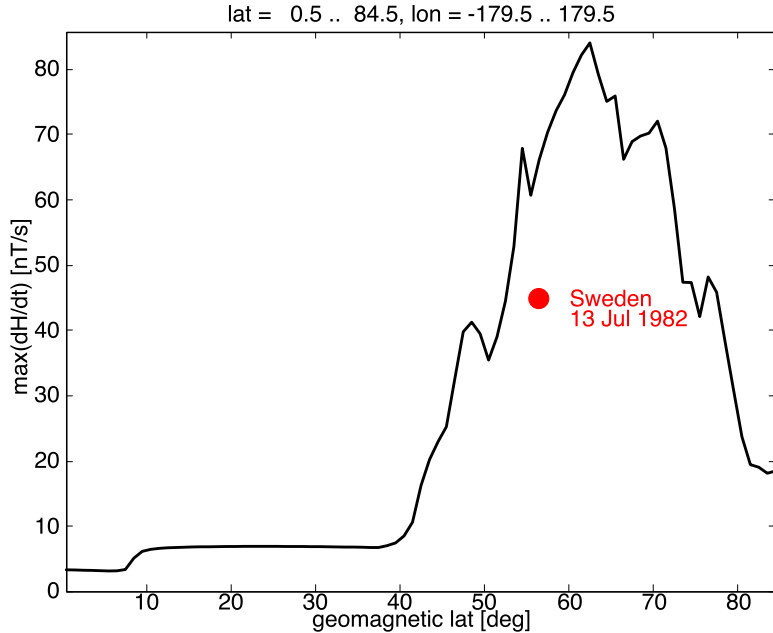


Figure 2: Largest value of the time derivative of the horizontal magnetic field vector in the northern hemisphere according to the Carrington event simulation. The red dot shows the largest known measured 1-min value at Lovö, Sweden, on 13 July 1982 (cf. Kappenman, 2005). Simulated magnetic field data are from the Community Coordinated Modeling Center (CCMC) run Elena_Marshalko_20211014_PP_1 based on the Blake et al. (2021) simulation (CARR_Scenario1 run at the CCMC), but with geomagnetic coordinates for the ground points.

4. DISCUSSION

Estimation of the strength of extreme ground magnetic field variations has a lot of practical importance. This is still a big challenge, since observations cover only quite a short period, so assessment of rare events has inevitable uncertainties. Simulations provide an alternative approach and they can give a global view. However, they are also prone to uncertainties due to incomplete description of relevant physics and they rely on assumptions of extreme conditions of the solar wind. So the results shown here must be understood as being very preliminary. Anyhow, the fast development of both space simulation and geomagnetic induction codes and increased computing power makes this a preferable way to proceed.

ACKNOWLEDGEMENTS

This work has been supported by the Academy of Finland grants no. 314670 and no. 339329.

REFERENCES

- Blake, S.P., A. Pulkkinen, P.W. Schuck, A. Glocer, D.M. Oliveira, D. Welling, R.S. Weigel and G. Quaresima, 2021. Recreating the Horizontal Magnetic Field at Colaba during the Carrington Event with Geospace Simulations. *Space Weather*, **19**, e2020SW002585, doi:10.1029/2020SW002585.
- Blake, S.P., A. Pulkkinen, P.W. Schuck, H. Nevanlinna, O. Reale, B. Veenadhari, and S. Mukherjee, 2020. Magnetic Field Measurements from Rome during the August-September 1859 Storms. *J. Geophys. Res. Space Phys.*, **125**, e2019JA027336, doi:10.1029/2019JA027336.
- Bolduc, L., 2002. GIC observations and studies in the Hydro-Québec power system. *J. Atmos. Sol.-Terr. Phys.*, **64**, 1793-1802, doi:10.1016/S1364-6826(02)00128-1.
- Clauer, C.R., and G. Siscoe, 2006. The great historical geomagnetic storm of 1859: A modern look. *Adv. Space Res.*, **38**, 117-118, doi:10.1016/j.asr.2006.09.001.
- Juusola, L., H. Vanhamäki, A. Viljanen, and M. Smirnov, 2020. Induced currents due to 3D ground conductivity play a major role in the interpretation of geomagnetic variations. *Ann. Geophys.*, **38**, 983-998, doi:10.5194/angeo-38-983-2020.
- Kappenman, J.G., 2005. An overview of the impulsive geomagnetic field disturbances and power grid impacts associated with the violent Sun-Earth connection events of 29-31 October 2003 and a comparative evaluation with other contemporary storms. *Space Weather*, **3**, S08C01, doi:10.1029/2004SW000128.
- Marshalko, E., M. Kruglyakov, A. Kuvshinov, L. Juusola, N.K. Kwagala, E. Sokolova, and V. Pilipenko, 2021. Comparing three approaches to the inducing source setting for the ground electromagnetic field modeling due to space weather events. *Space Weather*, **19**, e2020SW002657, doi:10.1029/2020SW002657.
- Myllys, M., A. Viljanen, Ø.A. Rui, and T.M. Ohnstad, 2014. Geomagnetically induced currents in Norway: the northernmost high-voltage power grid in the world. *J. Space Weather Space Clim.*, **4**, A10, doi:10.1051/swsc/2014007.

Geofysiikan Seura r.y. (perustettu 1926) edistää geofysiikan tutkimusta ja on sitä harjoittavien henkilöiden yhdyssiteenä. Geofysiikan aihepiirejä ovat maa, vesi, ilma ja lähiavaruus. Seuran toimintaan kuuluvat kaikille avoimet esitelmätilaisuudet ja *Geophysica*-lehden julkaiseminen. Seura järjestää useimmiten joka toinen vuosi Geofysiikan Päivät -kokouksen.

The Geophysical Society of Finland (founded in 1926) advances geophysical research and serves as a link between those involved in it. Geophysics focuses on the solid earth, water, atmosphere and near space. The Society arranges public lectures on different geophysical topics and publishes the journal *Geophysica*. Usually every second year it arranges a meeting titled Geophysics Days.